Alaska Division of Geological & Geophysical Surveys

Miscellaneous Publication 161

FIELD TRIP GUIDE: SEDIMENTOLOGY, RESERVOIR QUALITY, AND TECTONIC SETTING OF LATE MIOCENE–EARLY PLIOCENE GAS-BEARING FORMATIONS, UPPER COOK INLET, ALASKA

by

David L. LePain, Kenneth P. Helmold, Robert J. Gillis, Richard D. Reger, and Robert F. Swenson

2017

$4.00

Released by:

STATE OF ALASKA
DEPARTMENT OF NATURAL RESOURCES
Division of Geological & Geophysical Surveys
3354 College Road
Fairbanks, Alaska 99709-3707

Field Trip Guidebook

SEDIMENTOLOGY, RESERVOIR QUALITY, AND TECTONIC SETTING OF LATE MIOCENE–EARLY PLIOCENE GAS-BEARING FORMATIONS, UPPER COOK INLET, ALASKA

Division of Geological & Geophysical Surveys

Association of American State Geologists
108th Annual Meeting
Girdwood, Alaska
June 16, 2016

Division of Oil and Gas

Produced by

STATE OF ALASKA
Department of Natural Resources
DIVISION OF GEOLOGICAL & GEOPHYSICAL SURVEYS
3354 College Road | Fairbanks, Alaska 99709-3707
907-451-5010
dggspubs@alaska.gov
dggs.alaska.gov

COVER PHOTO: *Bluff exposures of the upper Beluga Formation near Bidarka Creek west of Homer; view toward the northwest. Photo by D. LePain, May 2008.*

Table of Contents

Figures

Tables

Sedimentology, Reservoir Quality, and Tectonic Setting of Late Miocene–Early Pliocene Gas-Bearing Formations, Upper Cook Inlet, Alaska

David L. LePain[1], Kenneth P. Helmold[2], Robert J. Gillis[1], Richard D. Reger[3], and Robert F. Swenson[4]

INTRODUCTION

This field trip provides an overview of the petroleum geology of Cook Inlet basin, with an emphasis on the sedimentology and reservoir quality of gas-bearing late Miocene and Pliocene strata of the Beluga and Sterling Formations. These formations are exposed in coastal bluffs between Soldotna and Homer on the Kenai Peninsula. The trip begins and ends at The Hotel Alyeska in Girdwood. A brief overview of the geology and tectonic setting of the basin will be presented on the motorcoach while en route to the first beach walk. The beach walks will be done in reverse stratigraphic order due to the timing of high and low tide at each location (table 1). The first beach walk will examine the upper Sterling Formation (early Pliocene) in bluff exposures at Clam Gulch, south of Soldotna. If the weather if good and sky is clear, the modern volcanic arc will be visible across the inlet, to the west. As its name suggests, Clam Gulch is a popular location for digging razor clams. Following the first beach walk, participants will re-board the motor coach for the one and one-half hour drive to Homer. To save time, the group will eat lunch on the bus while en route. The second beach walk will allow participants to examine the upper part of the Beluga Formation (late Miocene). On a clear day the Chugach Mountains are visible to the east and southeast, and the modern arc to the west.

The modern Cook Inlet estuary has the second highest tidal range in North America, second only to the Bay of Fundy in eastern Canada. Bluff exposures rimming the Kenai Lowland are best viewed during low tide when a wide, intertidal sand flat is subaerially exposed. The tides on June 16 are most favorable for a morning beach walk at Clam Gulch (table 1 and figure 1). We will arrive at that location approximately one hour after the low tide at 8:32 AM and should have enough time for a beach walk before the rising tide restricts our ability to walk along the beach. For this reason we have arranged our two beach walks in reverse stratigraphic order (youngest first, oldest last). Low tide at Homer is 7:02 AM and the high tide is 1:19 PM. We anticipate arriving in Homer around 2:00 PM, which will be roughly 40 minutes after high tide, so the water level will be falling and the beach area expanding.

This guidebook provides a brief introduction to the basin and an overview of the Beluga and Sterling Formations, followed by brief descriptions of the stratigraphy that will be seen during each beach walk.

Table 1. NOAA tide tables for June 16, 2016, for Homer and Cape Kasilof, Cook Inlet, Alaska.

Homer

	Time		Height	
	h m		ft	cm
16 Th	12:20	AM	15.9	485
	07:02	AM	1.8	55
	01:19	PM	14.0	427
	06:51	PM	4.5	137

Cape Kasilof

	Time		Height	
	h m		ft	cm
16 Th	02:01	AM	18.2	555
	08:32	AM	1.4	43
	02:52	PM	16.7	509
	08:42	PM	4.7	143

[1] Alaska Division of Geological & Geophysical Surveys, 3354 College Road, Fairbanks, Alaska 99709-3707; david.lepain@alaska.gov
[2] Alaska Division of Oil and Gas, 550 West 7th Avenue, Suite 1100, Anchorage, AK 99501-3560; ken.helmold@alaska.gov
[3] Reger's Geologic Consulting, PO Box 3326, Soldotna, AK 99669-3326; rdreger@acsalaska.net
[4] State Geologist, Emeritus, PO Box 2273, Homer, AK 99603; hmslena@gmail.com

Figure 1. *Shaded relief map of the Kenai Peninsula, showing the field trip route and the two beach walk locations.*

Although the focus of this trip is the Neogene coal-bearing section in outcrop and the petroleum geology of Cook Inlet basin, the modern sand flat exposed at low tide is a natural laboratory for sedimentologists, biologists, and anyone interested in nature. A wide variety of sea birds and large numbers of bald eagles can be seen most days, and large numbers of invertebrates live in the sandy substrate in the intertidal zone. A variety of wave, current, and combined-flow ripple bedforms are well developed and visible all around. You will have the opportunity to see these structures and observe how they are modified by changing water levels and a burrowing infauna.

This trip is co-led by Dave LePain (DGGS), Ken Helmold (DOG), Bob Gillis (DGGS), Bob Swenson (DGGS retired), and Dick Reger (DGGS retired and geology consultant).

REGIONAL GEOLOGY OF COOK INLET BASIN

Swanson River field, discovered in 1957, was the first commercially exploitable oil field found in the basin (figure 5; Hite and Stone, 2013). Since that time, 11 oil fields and 31 gas fields have been discovered. The main reservoirs are in Tertiary nonmarine rocks; a few fields (such as Granite Point) have produced some oil from Mesozoic rocks, but the total volume has been relatively minor. As a forearc basin, Cook Inlet basin is relatively unique in that only a small number of these basins around the world have known voluminous oil and gas accumulations that support commercial hydrocarbon production (Dickinson, 1995), let alone three petroleum systems as currently recognized in Cook Inlet. These three systems include a Mesozoic–Late Cretaceous oil system, a Mesozoic–Tertiary oil system, and a Tertiary microbial gas system (Claypool and others, 1980; Magoon, 1994). As of the end of 2010, more than 1.3 billion barrels of oil and about 8 trillion cubic feet of gas have been produced from the basin (Hite and Stone, 2013; LePain and others, 2013).

Cook Inlet is a complex collisional forearc basin that extends at least from the Shelikof Strait in the southwest, to the east end of the Matanuska Valley region in the northeast (figure 2). The basin is bounded on its west side by the Alaska–Aleutian range, a volcanic arc that has been active intermittently for at least the past 200 million years, and on its east side by the Chugach Mountains, one of the largest subduction complexes on the planet. The basin is divisible into three segments including, from southwest to northeast, lower Cook Inlet, upper Cook Inlet, and the Matanuska Valley. We define upper Cook Inlet, the focus of this field trip, as that part of the basin between the Augustine–Seldovia arch and the west entrance to the Matanuska Valley, and lower Cook Inlet as that part of the basin between the Augustine–Seldovia arch and the south end of Shelikof Strait. The Matanuska Valley represents the onshore, collapsed part of the basin that has been telescoped as a result of collision between the Yakutak microplate and mainland Alaska starting in Miocene time (Trop and Ridgway, 2007).

The modern Cook Inlet estuary is situated along the axis of the forearc sedimentary basin. Discontinuous exposures of Mesozoic and Tertiary rocks are present along the east and west sides of the basin; the upper part of the Tertiary section (late Miocene and early Pliocene) is exposed in low bluff exposures that rim the Kenai Lowland. A subsurface dataset that includes two-dimensional (2-D) seismic and a limited number of exploration wells penetrating Mesozoic rocks demonstrate the Mesozoic section extends continuously under the basin from northwest to southeast (Fisher and Magoon, 1978; figure 3). The basin includes a composite thickness of dominantly marine Mesozoic strata totaling more than 35,000 feet (~10,670 m) thick (figure 4; Detterman and Hartsock, 1966; Kirschner and Lyon, 1973). These rocks include the record of an Early Jurassic oceanic arc (Talkeetna arc) that formed a significant distance south of its present latitude (Nokleberg and others, 1998) and, starting in Middle Jurassic time, the sedimentary record of the gradual exhumation of that arc (Detterman and Hartsock, 1966; Trop and others, 2005; Trop and Ridgway, 2007). The presence of tuffs in the upper part of the Kamishak Formation likely record the onset of Talkeetna arc volcanism in latest Triassic time (Wang and others, 1988; Rioux and others, 2010). Lower Middle Jurassic rocks are thought to have sourced the oil in upper Cook Inlet oil fields (Magoon, 1994). The oceanic arc ultimately collided with the continental

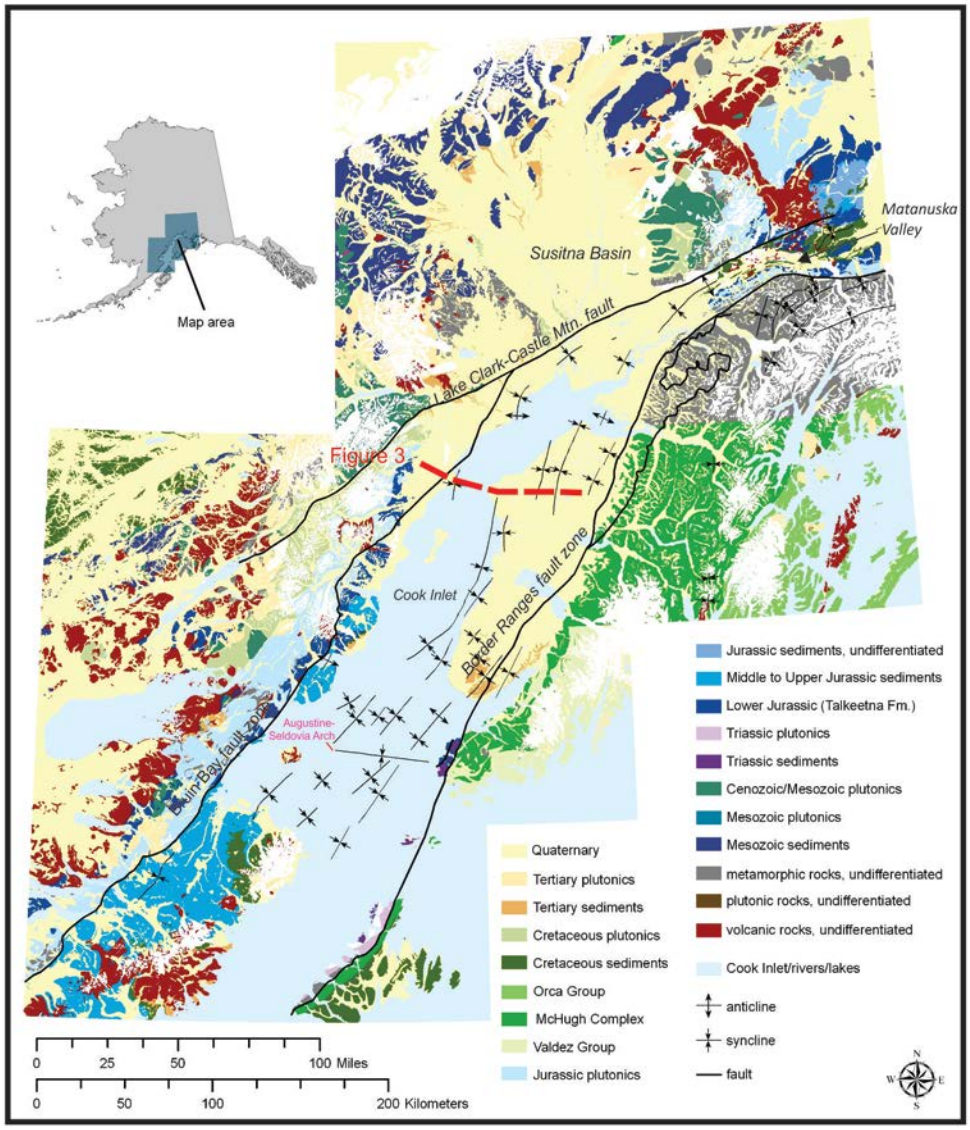

Figure 2. *Generalized geologic map of the Cook Inlet region. The red dashed line extending across Cook Inlet shows the location of the cross-section in figure 3. Modified from Wilson and others (2012).*

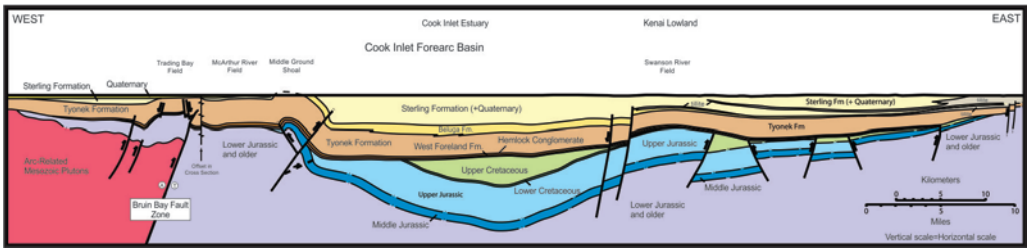

Figure 3. *Geologic cross-section showing generalized structure and stratigraphy in upper Cook Inlet basin. Modified from Haeussler and others (2000) and Boss and others (1976).*

backstop of North America south of its present-day location in the Late Jurassic to Cretaceous and was subsequently translated northward along large-scale strike-slip fault systems. In this process the arc and forearc regions were converted to the continental margin tectonic elements seen today.

Regional uplift in latest Cretaceous–earliest Tertiary time terminated marine deposition in the basin and resulted in a basin-wide unconformity that separates Tertiary nonmarine strata from Mesozoic rocks (figure 4; Calderwood and Fackler, 1972; Boss and others, 1976). Shellenbaum and others (2010) have mapped this surface, providing a good estimate of the thickness of Tertiary strata throughout the basin (figure 5). The Tertiary succession is nonmarine and greater than 25,000 feet (~7,620 m) thick about 30 miles (48 km) north of Clam Gulch, in the vicinity of Nikiski (figures 4 and 5; Kirschner and Lyon, 1973; Calderwood and Fackler, 1972; Boss and others, 1976). Microbial processes operating on coal-bearing Miocene and Pliocene rocks likely generated most of the gas in upper Cook Inlet fields (Claypool and others, 1980). Fluvial sandstones of this age are the main gas reservoirs in the basin.

Major crustal-scale fault systems bound the basin on its west and east sides and separate it from a magmatic arc and subduction complex (Bruin Bay and Border Ranges fault systems, respectively; LePain and others, 2013; Swenson, 2003; figure 2). The basin is bounded on its north side by the dextral strike-slip Castle Mountain fault system. This fault system separates the forearc basin from the less-well-known Susitna basin to the north.

This field trip focuses on the sedimentology, sand-body geometries, reservoir quality, and petroleum geology of the late Miocene Beluga Formation and latest Miocene to early Pliocene Sterling Formation in outcrop along the west and south shores of the Kenai Lowland (figures 1 and 4). Calderwood and Fackler (1972) redefined the stratigraphic nomenclature for the Tertiary stratigraphy of the basin, which is generally accepted and in widespread use today. Due to limited exposures, these authors designated subsurface type sections for all Tertiary formations in the basin (figure 6). As expected in an active nonmarine forearc basin, the Tertiary stratigraphy is complex, and dramatic facies changes over relatively short distances are the norm, rather than the exception (LePain and others, 2013; Swenson, 2003). Lithofacies and biostratigraphic datasets throughout the northern part of the basin demonstrate the time-transgressive, gradational nature of Cenozoic formations.

The older Tertiary formations (Tyonek—Oligocene to middle Miocene; Hemlock—late Eocene(?) to late Oligocene; and West Foreland—Eocene) will not be addressed on this trip. The following sections provide a description of the Neogene forearc basin stratigraphy we will examine on this field trip.

NEOGENE FOREARC BASIN STRATIGRAPHY

Neogene strata in Cook Inlet basin include most of the Tyonek Formation (early to middle Miocene), the late Miocene Beluga Formation, and the latest Miocene to early Pliocene Sterling Formation (figure 4). Outcrop data suggest the Tyonek is Oligocene to middle Miocene. The Tyonek Formation is not exposed on the Kenai Lowland and will not be discussed further in this guidebook. For a discussion of the Tyonek Formation see Flores and others (1994, 1997, 2004) and LePain and others (2008, 2013).

Beluga Formation

Type Section and Age

Calderwood and Fackler (1972) named a 4,150-foot-thick succession of interbedded claystone, siltstone, sandstone, and lignitic to subbituminous coal the Beluga Formation and designated the interval between the depths of 3,610 and 7,760 feet (1,100–2,365 m) in the Standard Oil of California Beluga River No. 312-35 well as the type section (figure 6). A distinctive feature of the formation in the type section is the lack of thick sandstones and coal seams, which are so characteristic of the underlying Tyonek Formation. Log correlations show that the unit is thickest in the area around the type well, is considerably thinner at Swanson River oil field, and is

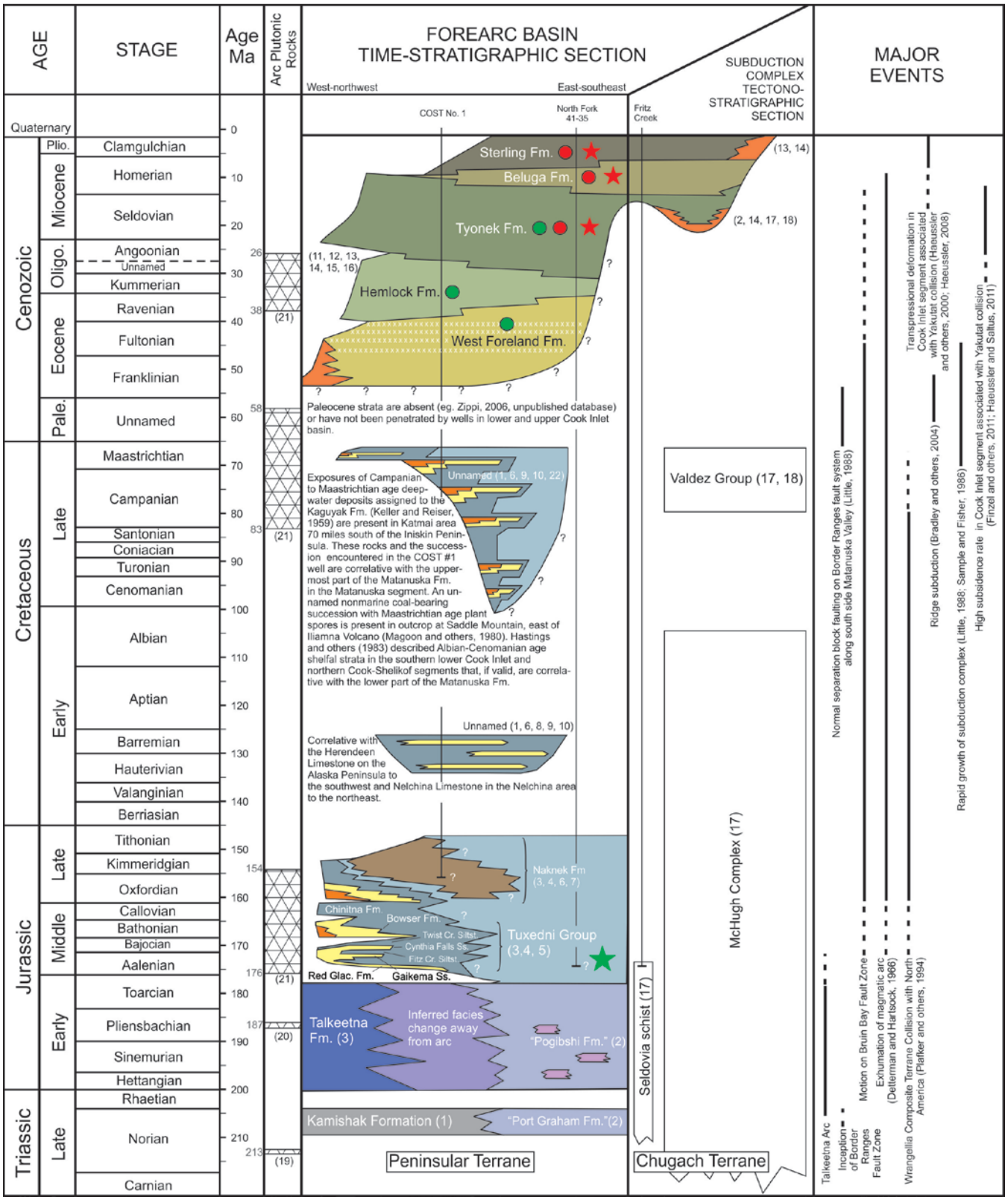

Figure 4. *Simplified chronostratigraphic column for Cook Inlet basin. Oil source rocks are shown with green star; gas source rocks (coal seams) are shown with red stars. Oil and gas reservoirs are shown with green and red circles, respectively. Based on unpublished industry and DGGS data.*

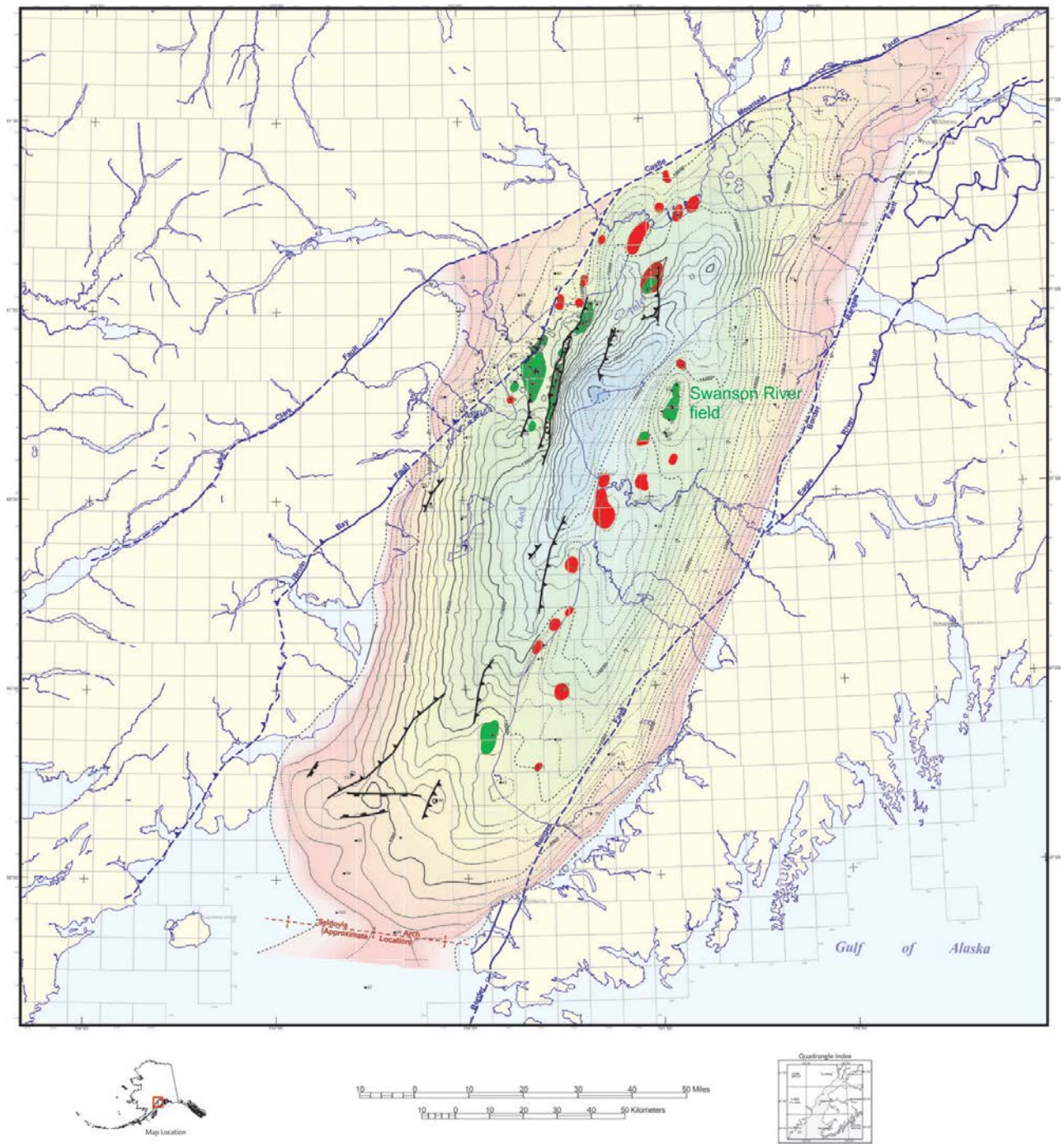

Figure 5. *Depth structure on the basal Tertiary unconformity surface. Contour interval 1,000 feet. Oil fields are shown in green and gas fields in red. Modified from Shellenbaum and others (2010).*

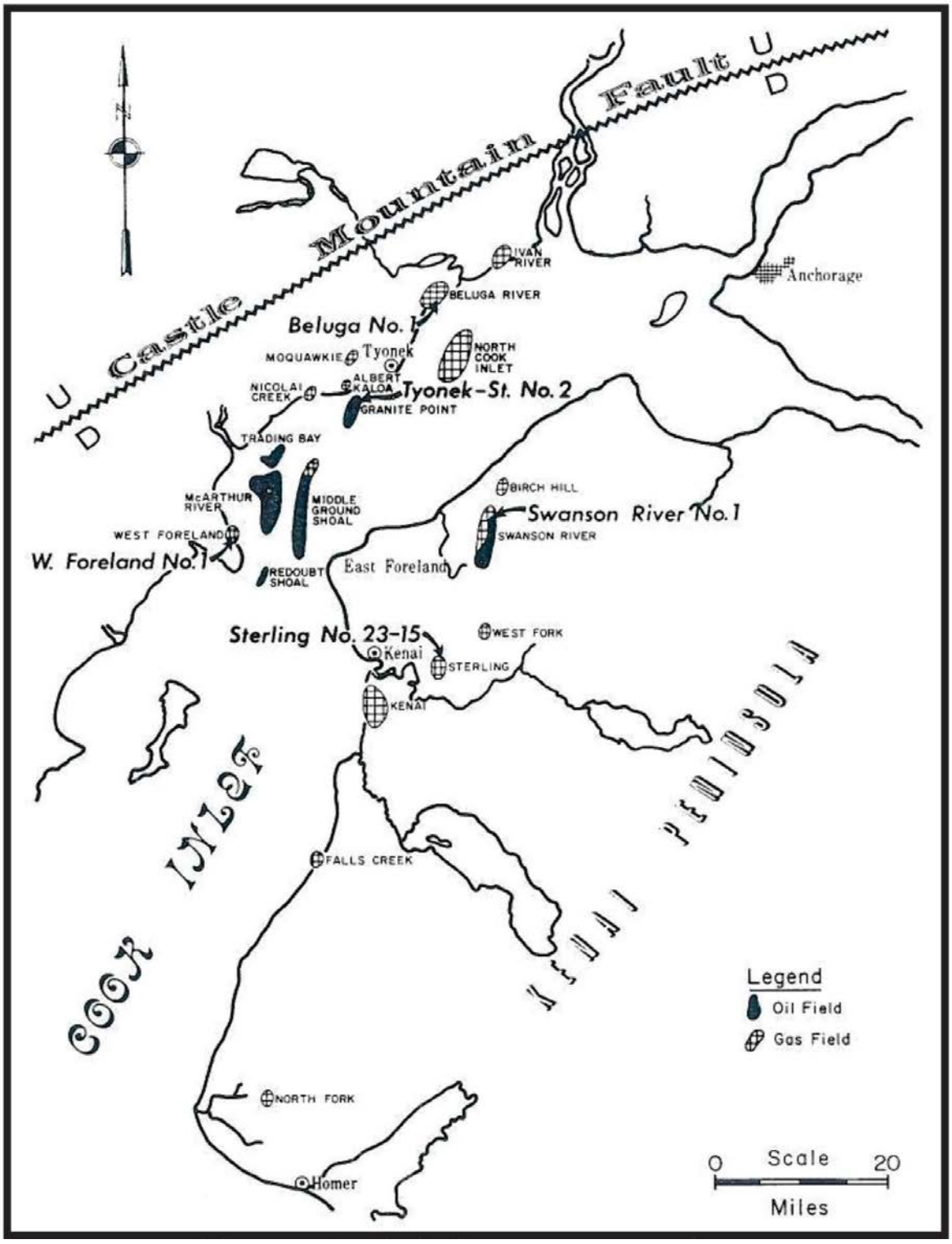

Figure 6. Map of upper Cook Inlet, showing locations of subsurface type sections for the Kenai Group. Modified from Calderwood and Fackler (1972).

missing locally in the northeastern part of the basin, where the Sterling Formation (early Pliocene) overlies Mesozoic rocks (Calderwood and Fackler, 1972). Boss and others (1976) noted the Beluga consists largely of floodplain shales and minor interbedded coal seams and channel sandstones. These authors recognized tillites in the unit on the east side of the basin, but did not provide details (figure 3). In outcrop along the southern Kenai Peninsula, the unit is gradationally overlain by the Sterling Formation. Sandstone bodies in the Beluga are important gas reservoirs in upper Cook Inlet.

Correlating Tertiary nonmarine formations in Cook Inlet basin is challenging due to the lack of suitable marker beds and robust age control. Calderwood and Fackler (1972) correlated their type Beluga with outcrops in the Homer area on the southern Kenai Lowland. These outcrops were assigned to the Homerian floral stage and considered late Miocene by Wolfe and others (1966). On the northwest side of the basin, Homerian pollen has been recovered from the Beluga Formation exposed along the Beluga and lower Chuitna rivers (Adkison and others, 1975; DGGS, unpublished data). ARCO considered the age of the Beluga to range from late early Miocene to late Miocene (Swenson, 2003).

Isotopic age dates for the Beluga Formation are in general agreement with biostratigraphic data. Coal seams in the Beluga commonly include highly disrupted volcanic ash layers (tonsteins). K/Ar dates on plagioclase grains extracted from ash layers in coals from the middle and upper parts of the formation in the Homer area range from 11.3 ± 0.7 Ma to 8.8 ± 0.9 Ma, respectively (Triplehorn and others, 1977; Turner and others, 1980). Results from $^{40}Ar/^{39}Ar$ dates on plagioclase grains extracted from disrupted ash layers in coal seams in a similar stratigraphic position exposed in the bluffs northwest of Homer range from 9.35 ± 0.62 Ma to 4.57 ± 0.72 Ma (Dallegge and Layer, 2004). The young end of this range suggests the presence of the Sterling Formation at that sample location. Detrital zircon data for two samples collected from the upper part of the Beluga Formation west of Homer, from outcrops we will see during our second beach walk, yielded weighted means of 9.77 Ma (± 0.73 Ma) and 9.07 Ma (± 0.52 Ma) on the youngest nine and five grains, respectively (DGGS, unpublished data). Maximum stratigraphic ages for the Beluga in outcrop on the west side of the basin ranges from 13.4 to 11.8 Ma (middle Miocene; DGGS, unpublished data).

Stratigraphy and Sedimentology

Numerous high-angle faults cut exposures of the Beluga Formation on the southern Kenai Lowland, complicating correlation between outcrops. Available biostratigraphic data suggest that the lower part of the Beluga is exposed in the low bluffs southeast of Anchor Point; the middle part of the formation is exposed in the bluffs near Fritz Creek, on the west shore of Kachemak Bay, northeast of Homer; and the upper part of the Beluga is exposed in the bluffs extending from Homer to the northwest, at least as far as Diamond Gulch (figure 1; Adkison and others, 1975). Exposures of the upper Beluga will be examined on this field trip during the second beach walk.

Exposures of the lower Beluga Formation near Anchor Point consist dominantly of clayey siltstone, siltstone, carbonaceous siltstone, minor claystone, lignitic to subbituminous coal seams, and thin, tabular-bedded, very-fine- to fine-grained argillaceous sandstones. This lower part of the Beluga records deposition in a poorly drained overbank setting, with only occasional influxes of coarser sediment as minor crevasse splays (distal end of sandy splay lobes). Exposures of the middle Beluga near Fritz Creek consist of similar muddy lithologies and coal seams up to 10 feet (3 m) thick, but also include locally prominent lenticular bodies of very-fine- to fine-grained sandstone up to 30 feet (9 m) thick encased in these finer-grained deposits (figure 7a). Multiple lenticular sand bodies are commonly observed at the same stratigraphic level. The middle Beluga at this location records deposition in a poorly drained overbank setting that was traversed by small to moderate sized, single-thread channels (anastomosing) through which very-fine- to fine-grained, muddy sand was transported. These locations will not be visited during this field trip.

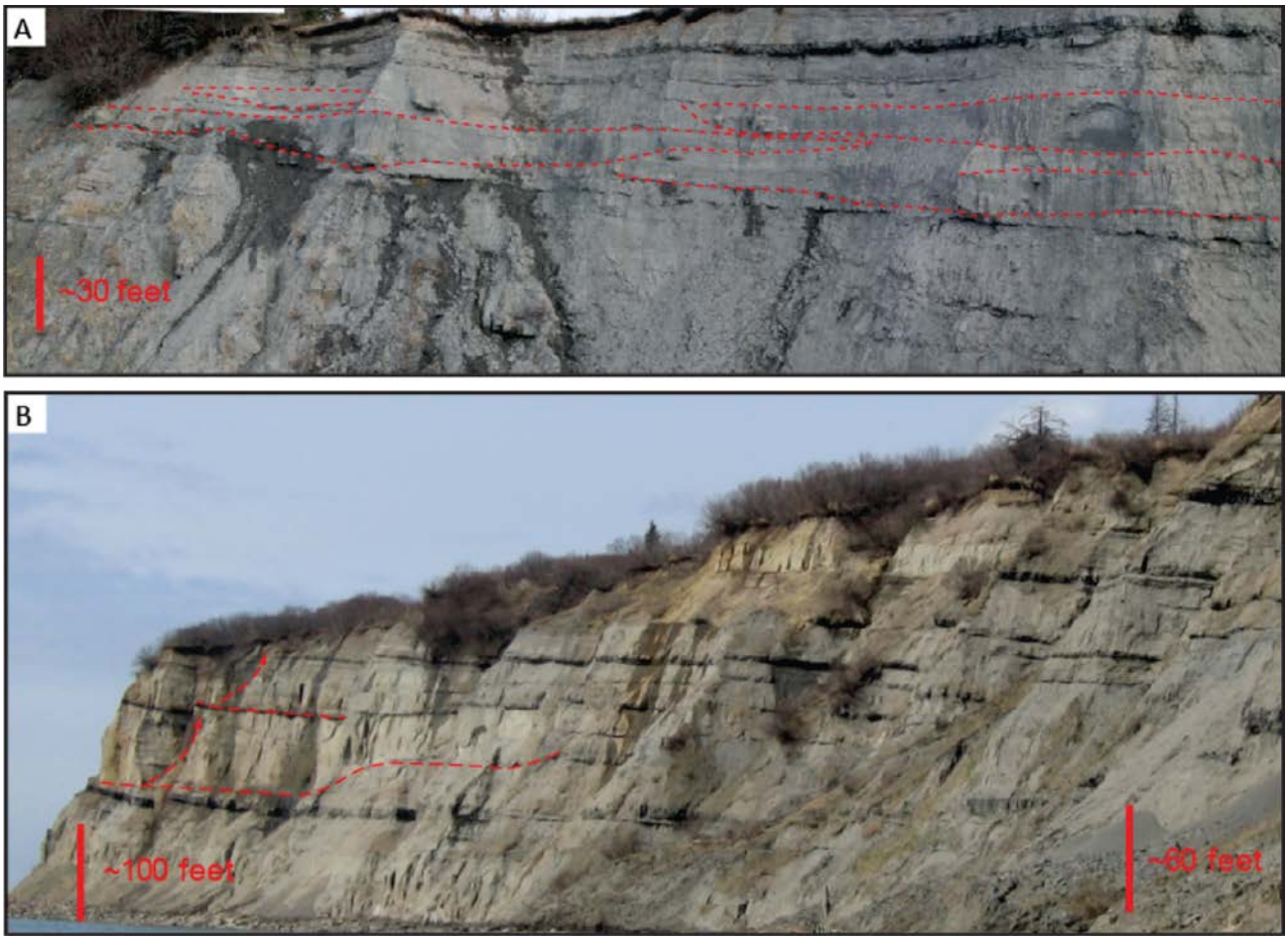

Figure 7. A. Photomosaic showing sand-body geometries in the middle part of the Beluga Formation exposed in bluffs along the west side of Kachemak Bay, near Fritz Creek. Dashed red lines outline channel-fills of muddy, very fine- to fine-grained sandstone. B. Bluff exposures of the upper part of the Beluga Formation near Bidarka Creek, west–northwest of Homer. Note the lateral continuity of coal seams in overbank mudstone succession and the broadly lenticular sand body. Dashed red line marks the base of a channel sand body. The dashed arrows mark show the vertical extent of two channel-fill sand bodies.

Exposures of the upper Beluga between Homer and Diamond Gulch include moderate to thick mudstone successions, including coal seams up to 7 feet (2.1 m) thick, and multiple broadly lenticular to sheet-like bodies more than 50 feet (> 15 m) thick of very-fine- to medium-grained sandstone (figure 7b). Sand bodies include discontinuous basal mudclast lags overlain by trough and planar cross-bedded sandstone in sets that range from 0.5 to 4 feet (0.15–1.2 m) thick; horizontally laminated sandstone is also common (figure 8a-c). Coalified plant material is common near the base of foreset laminae and drapes some horizontal laminae. Convolute bedding is common and includes deformed horizontally laminated and cross-bedded sandstones. Mudstones are typically massive, but horizontally laminated mudstones are relatively common. Coal is sub-bituminous and woody fragments are clearly visible (figure 8d-e). The composition of sandstones in the Beluga is discussed below.

The upper Beluga near Homer records deposition in poorly drained overbank settings that were traversed by relatively large rivers that transported a mixed load of sand and mud. These rivers are interpreted to be part of an axial–fluvial system. These sand bodies will be visible in the distance during our Homer beach walk (figure 7b). Recent work on the sedimentology and reservoir potential of the Beluga Formation is summarized in LePain and others (2008), LePain and others (2009), LePain and others (2013), Mongrain (2012), and Helmold and others (2013). Previous studies by Hayes and others (1976), Rawlinson (1984), and Flores and Stricker (1992) also address the sedimentology of the formation.

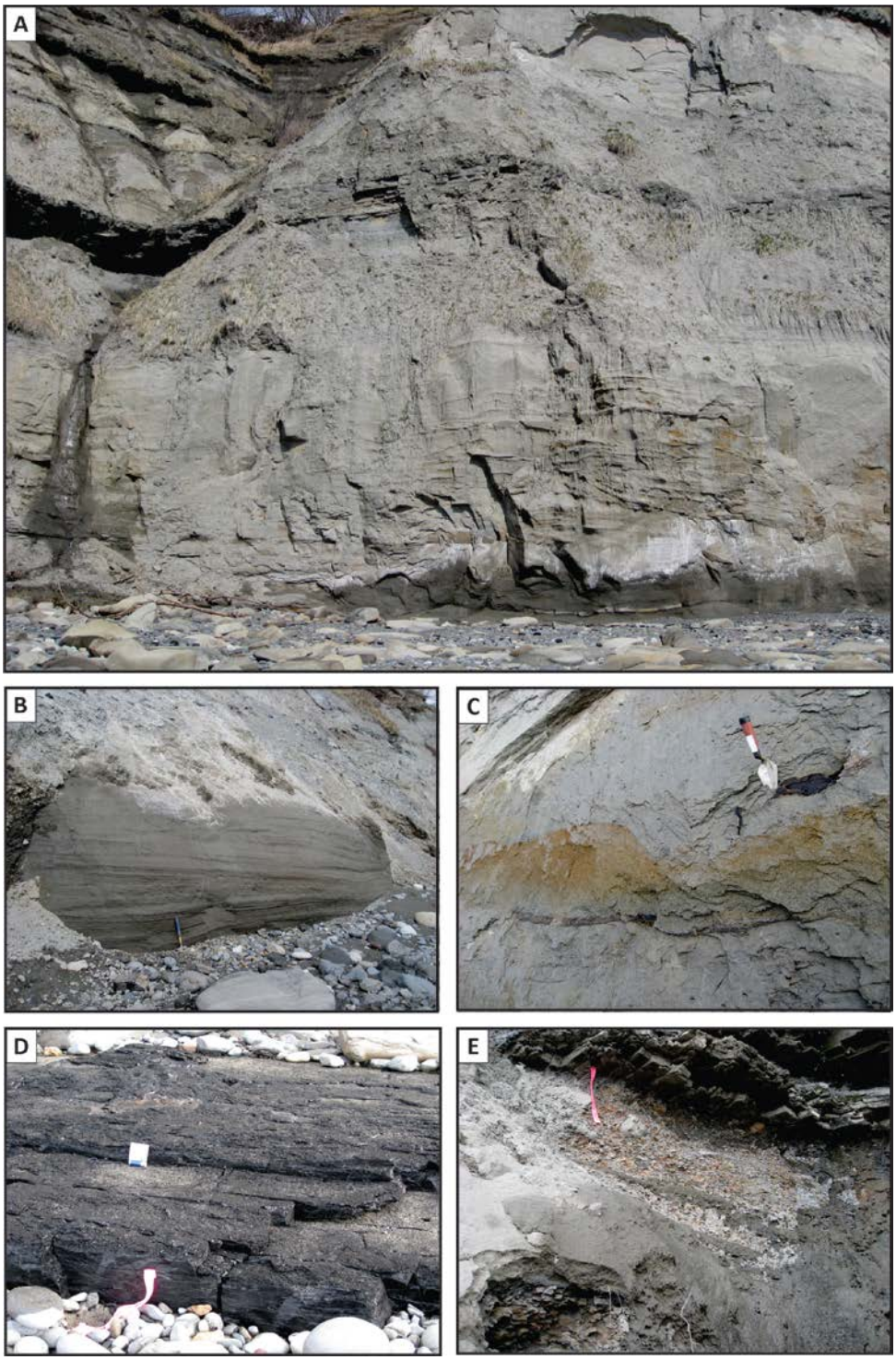

Figure 8. *A. Sand body exposed at the base of the bluff west of Bidarka Creek. Note the internal facies architecture of the sand and the overlying mudstone package. The sand body is composed of stacked sets of cross-bedded sand and interbedded horizontally laminated sand. These facies are truncated at several locations in the body by scour surfaces. B. Low-angle laminae in sand overlain by low-angle laminae dipping in the opposite direction (apparent dip). These probably represent stacked sets of trough cross-bedded sand. C. Cross-bedded sand that originated from the migration of 2-D bedforms. D. Subbituminous coal seam exposed at beach level (measured section 08DL001, see figure 23). E. Angular, blocky weathering mudstone below coal seam at the top of measured section 08DL001 (figure 23).*

Soft-Sediment Deformation and Liquefaction Features—Soft-sediment deformation features are locally prominent in sands of the Beluga, but they are not as common in outcrop as in the overlying Sterling Formation. This may be more apparent than real. Due to environmental conditions not clearly understood the upper part of a sand body exposed at beach level northwest of Homer, referred to informally as the Shellenbaum sand, was washed clean of slope wash and near-surface interstitial clay when visited in May 2008, revealing fine-scale internal structures (figure 9).

The exposed part of the Shellenbaum sand (0–3.4 m [0–11.2 ft] in measured section shown in figure 9) consists of fine-grained sand and includes a variety of sedimentary structures, including plane-parallel lamination, trough cross-lamination, trough cross-bedding, and convolute bedding. The lowermost exposed sand bed forms a wave-cut surface roughly parallel to depositional horizontal and represents a horizontal slice through small-scale trough cross-laminae (rib and furrow structure of Pettijohn and Potter, 1964). This sand bed is overlain by a prominent plane-parallel laminated sand bed up to 4 feet (1.2 m) thick comprising alternating dark brown to black laminae up to 0.25 inches (0.64 cm) thick with abundant macerated plant fragments, and medium-gray laminae up to 1 inch (2.5 cm) thick consisting dominantly of siliciclastic material. These parallel laminae grade laterally to trough cross-bedded sandstone in which the base of some foresets are lined with plant material. Farther along strike in the same bed, trough cross-bedded sandstone grades to convolute-bedded sandstone with upright and overturned disharmonic anticlinal and synclinal folds. At several locations in the bed, laminae can be traced laterally to abrupt terminations against vertically oriented pipe-like structures filled with massive, fine-grained sandstone (figure 9). At some locations the sand-filled pipes are near the crest of anticlinal folds. Platy shaped plant fragments (‘corn flakes’) line the margin of at least one pipe structure. Elsewhere in the outcrop, plane-parallel laminae and low-angle cross-laminae grade laterally over a few inches to internally massive zones. In several examples of this, the massive zones were immediately below vertically oriented pipe-like features filled with massive sandstone—the lower ends of pipes terminated at the top of the underlying massive zones, and massive sand can be traced without break from one to the other. The upper ends of most pipes are truncated by erosion surfaces at the base of overlying beds. Three to four feet (0.9–1.2 m) above the base of the exposure convolute-bedded sandstone consists of deformed scours (apparent scour widths > 6 feet [> 1.8 m] and ≤ 2 feet [0.6 m] deep) that are filled with low-angle foresets that dip consistently in one direction (southeast), representing deformed large-scale trough cross-beds. Due to the weathering characteristics typical of most Beluga exposures, in which most fine-scale sedimentary structures are covered with slope wash, we do not know how common these features are in the unit.

Soft-sediment deformation features and closely associated structureless sandstone masses, including the vertically oriented pipe-like structures filled with massive sandstone, strongly suggest linked origins. The abrupt termination of physical sedimentary structures (such as plane-parallel lamination and cross-bedding) against structureless sandstone in the same beds indicates original sedimentary structures were destroyed as localized parts of beds became liquefied. Liquefaction features appear to be associated with the axial region of soft-sediment folds, suggesting folding and liquefaction were linked and were a response to the same driving mechanism. Pore fluid flow may have been focused in the axial region of folds, leading to greater potential for liquefaction there.

The association of convolute bedding and features suggestive of liquefaction processes are interpreted to be the result of cyclic loading due to major earthquakes. Convolute bedding is relatively common in many fluvial successions from a wide variety of tectonic settings where it is the result of processes inherent to the fluvial systems (such as rapid deposition during high flow events and subsequent deformation possibly associated with fluid drag forces at the sediment–water interface). Given the tectonically active forearc basin setting of Cook Inlet, a seismogenic origin is most compelling.

08DL004
"Shellenbaum" sand, Seldovia C-5
N59.64523 W151.60587
Beluga Formation

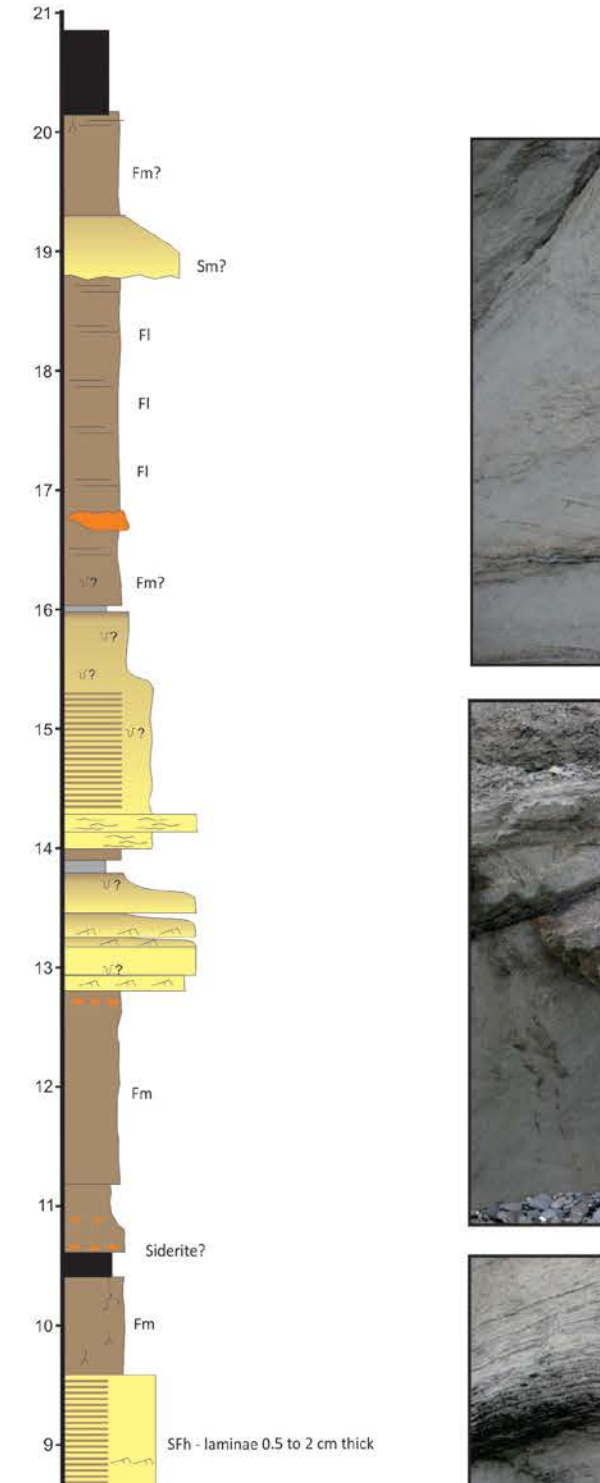

Facies Codes
Sm - massive sandstone
Sp - planar-tangential cross-bedded sandstone
Sr - ripple cross-laminated sandstone
Scb - convolute bedded sandstone
SFh - interbedded sandstone and mudstone (heterolithic)
Fm - massive mudstone
Fl - laminated mudstone
Fr - ripple cross-laminated mudstone

Convolute bedded sandstone at 1.2 m in measured section. Bed consists of deformed planar-tangential cross-bedding.

Fluid escape pipe filled with massive sandstone at 0.6 m in measured section. Platy shaped plant fragments line the margins of the pipe.

Convolute bedded sandstone at 0.0 m in measured section. Note massive sandstone near head of hammer. Dark laminae have abundant woody plant fragments.

Bedding-parallel cut through trough cross-laminae, referred to as rib and furrow structure. Exposed at beach level (0.0 m in measured section).

Figure 9. *Measured section in the upper Beluga Formation, west of Bidarka Creek. The informally named "Shellenbaum sand" forms the base of the section (0 to 3.4 m). Convolute bedding and liquefaction features are well preserved in this sand body.*

Beluga–Sterling Contact

The contact between the Beluga and Sterling Formations is gradational and well expressed along the west shore of Kachemak Bay by a gradual upsection increase in sand-body thickness and lateral continuity, and a decrease in the thickness of mudstone successions and coal seams over a stratigraphic thickness of several hundred feet. Coal beds thicker than 1 foot (0.3 m) gradually become less abundant (Adkison and others, 1975) and sandstones become less clayey. These changes persist into the overlying Sterling Formation. Along the Beluga River a thick mudstone succession in the Beluga Formation transitions to thick, tabular sandstones with relatively thin interbedded mudstones over what appears to only a few hundred feet. In addition to these changes there is a significant upsection change in sandstone composition from Beluga to Sterling (discussed below).

Composition and Reservoir Quality of Sandstones in the Beluga Formation

Sandstones of the Beluga Formation are somewhat unique in that they contain relatively small amounts of quartzose grains (monocrystalline and polycrystalline quartz including chert). Instead, they are enriched in argillaceous sedimentary and metasedimentary detritus with an average modal composition of $Q_{28}F_{10}L_{62}$, $Q_{m8}F_{10}L_{t82}$, $Q_{m53}P_{40}K_{7}$, $Q_{p25}L_{vm15}L_{sm60}$ (figure 10). The average grain size is 0.26 mm (lower medium) with an average Folk sorting of 1.27 (poor; figure 11a). The sandstones consist largely of argillaceous lithic grains including mudstone (figure 12e), siltstone (figure 12d), argillite, and phyllite, resulting in high structural-clay content. Quartz, feldspar and chert (figure 12f) are minor components of the rocks, together comprising less than one-quarter of the framework fraction. Intergranular volumes (IGVs) average 22 percent, indicating the rocks have undergone moderate compaction (figure 12a-b). The Beluga sands are one of the main gas reservoirs in Cook Inlet with the most productive horizons having porosities in excess of 25 percent and permeabilities of several hundred millidarcies (figure 13). The effective porosity of the rocks might be significantly lower than the measured values due to the prevalence of microporosity in the argillaceous lithic fragments. Because of the small pore throats associated with the micropores, the migration of liquids, particularly liquid hydrocarbons, may be retarded. Subsurface data document the existence of poorer quality Beluga sands (porosities less than 15 percent and permeabilities less than 1 millidarcy) that are most likely finer-grained, lower-energy overbank deposits. Cementation is not significant, with total cements averaging less than 2 percent of the bulk rock. Due to high clay content they are readily susceptible to ductile grain deformation (figure 12b-c).

The sands were most likely derived from sedimentary and metasedimentary rocks of Mesozoic age in the Chugach terrane, east of the Cook Inlet basin, with additional contributions from the Kahiltna assemblage, north and west of the basin. With the ambiguities of identifying mudstones via standard petrographic techniques, it is difficult to assess the extent of contributions from the two sources.

Sterling Formation

Type Section and Age

Calderwood and Fackler (1972) named a 4,490-foot-thick (1,369-m-thick) succession of massive sandstone, conglomeratic sandstone, and claystone the Sterling Formation and designated the interval between 1,050 and 5,540 feet (320–1,689 m) in the Union Oil Company of California 23-15 well, the discovery well in the Sterling gas field, as the type section (figure 6). Lignitic coal seams and coaly streaks are common. Seams tend to be thinner (1–3 feet [0.3–0.9 meters]) than in the Beluga Formation, rarely achieve a thickness of 8 feet (2.4 m), and typically have high ash content. Calderwood and Fackler (1972) noted that well and seismic data suggest the formation is approximately 11,000 feet (~3,350 m) thick in the East Foreland area. Sandstone bodies in the Sterling are important gas reservoirs in upper Cook Inlet.

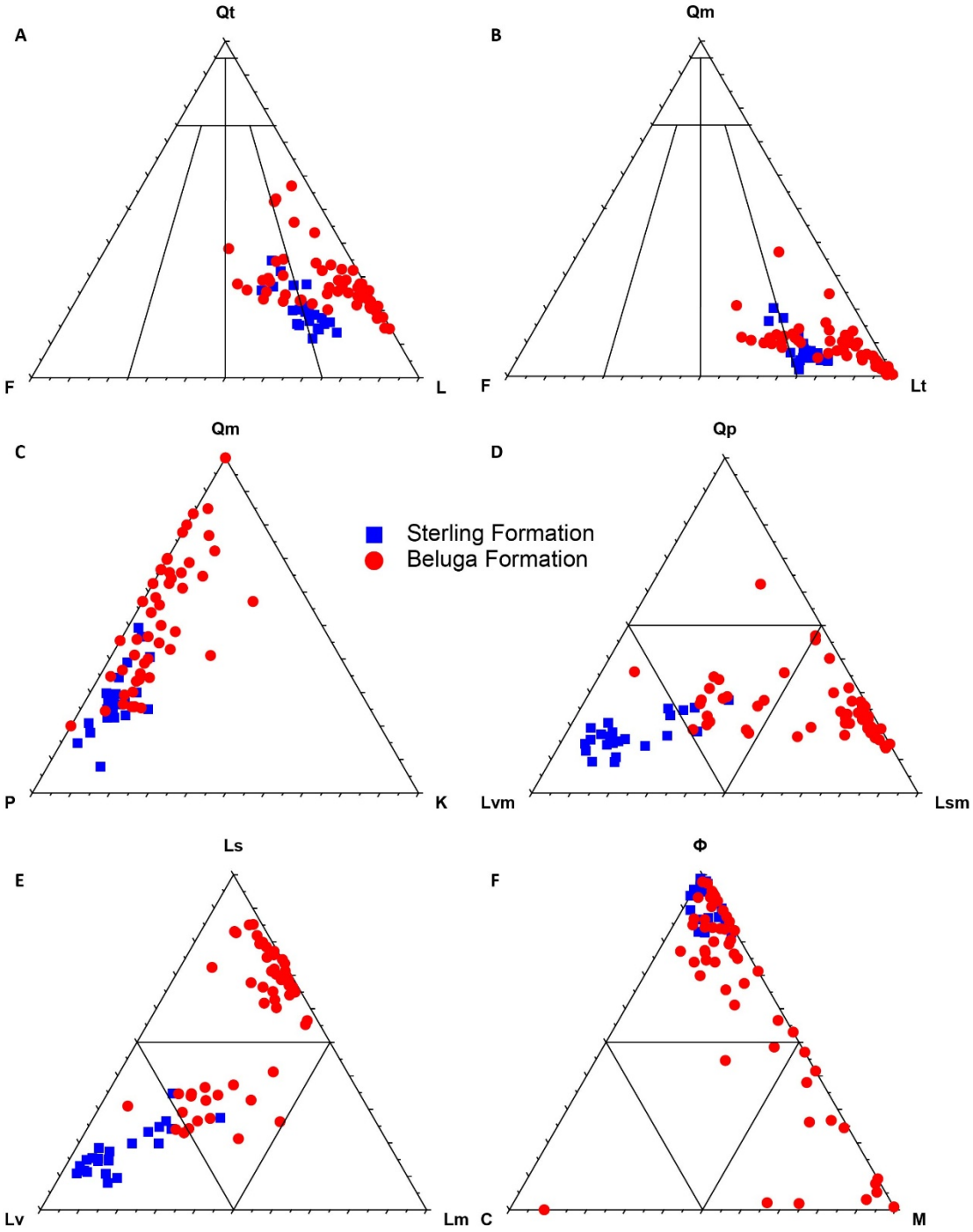

Figure 10. Ternary diagrams, showing composition of Beluga and Sterling sandstones. The data were obtained via the traditional point-counting method in which phaneritic rock fragments are classified as the appropriate lithology (for example, granite, diorite, gabbro, gneiss). See table 2 for explanation of grain and intergranular parameters used in the diagrams. A. QtFL diagram; both Beluga and Sterling sands are relatively enriched in lithic detritus. B. QmFLt diagram; both Beluga and Sterling sands contain only minor quantities of monocrystalline quartz. C. QmPK diagram; Sterling sands have high P/F ratios, reflecting derivation from volcanic rocks. D. QpLvmLsm diagram; Beluga and Sterling sands are clearly distinguished by the high content of sedimentary versus volcanic rock fragments, respectively. E. LsLvLm diagram; volcanic and sedimentary rock fragments are the dominant types of lithic grains. F. ΦCM diagram; most Sterling and Beluga sands have significant reservoir potential.

Table 2. *Classification of Grain and Intergranular Parameters (modified from Dickinson, 1985).*

A. Quartzose grains
- Q_m = Monocrystalline quartz
- Q_p = Polycrystalline quartz (including chert)
- Q = Total quartzose grains (Q_m + Q_p)

B. Feldspar grains
- P = Plagioclase
- K = Potassium feldspar
- F = Total feldspar grains (P + K)

C. Lithic grains
- L_s = Sedimentary rock fragments (including chert)
- L_v = Volcanic rock fragments
- L_m = Metamorphic rock fragments
- L_p = Plutonic rock fragments
- L_{sm} = Sedimentary and metasedimentary rock fragments
- L_{vm} = Volcanic and metavolcanic rock fragments
- L = Lithic grains (L_s + L_v + L_m + L_p)
- L_t = Total lithic grains (L + Q_p)

D. Intergranular components
- Φ = Total porosity
- C = Total cement
- M = Matrix + clay laminae/burrows

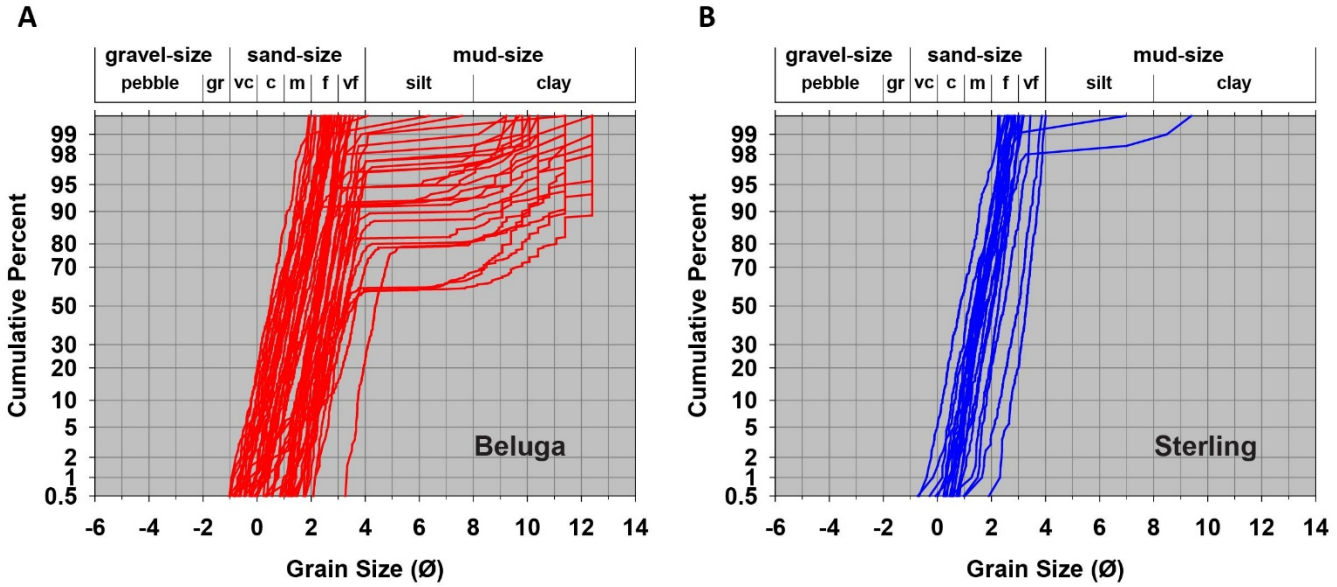

Figure 11. *Cumulative probability plots of grain size by unit. Sediments with a normal (Gaussian) distribution plot as a straight line. The value of the 50th percentile indicates grain size while the slope of the line indicates sorting. A. Beluga Formation. B. Sterling Formation.*

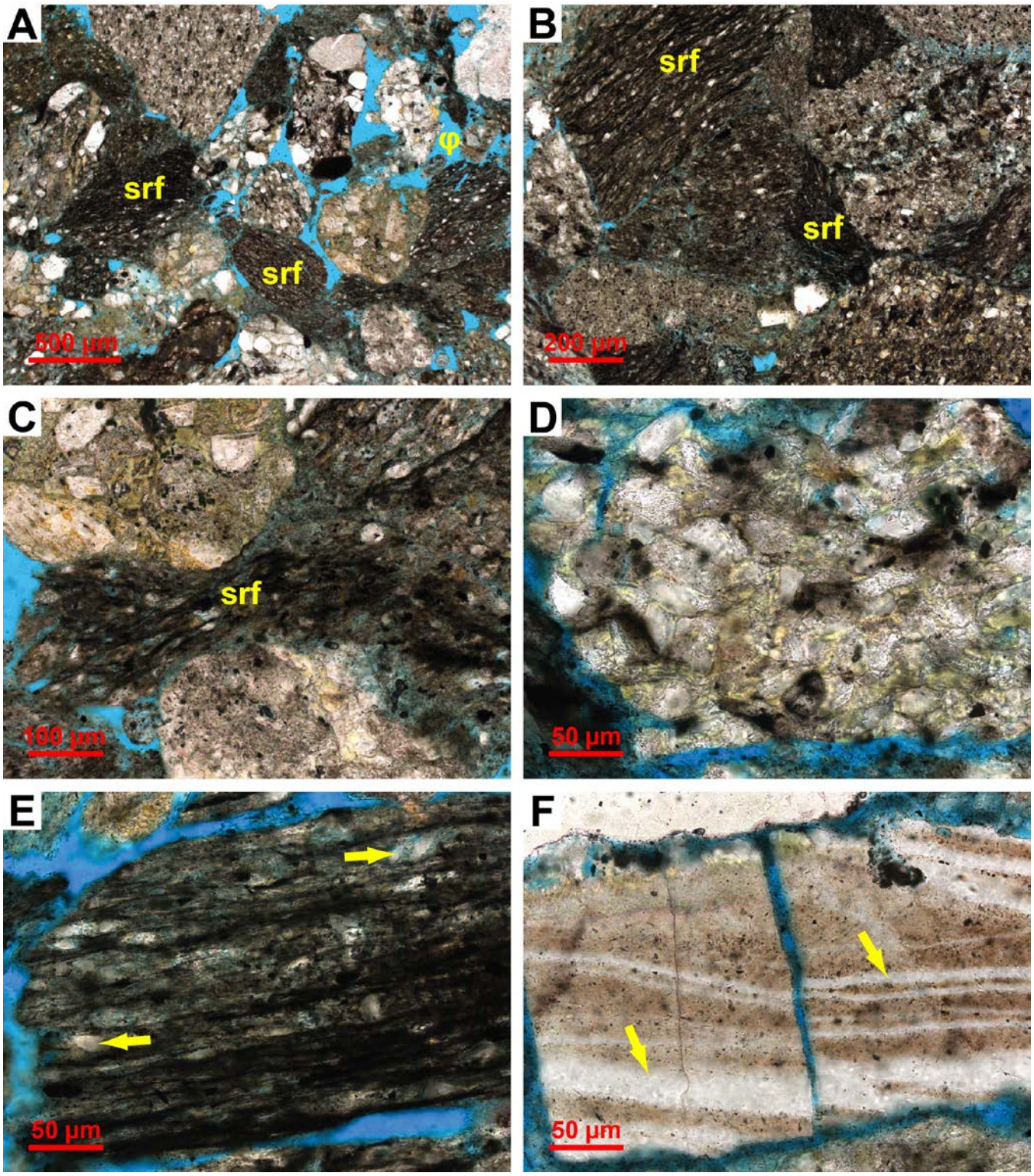

Figure 12. *Photomicrographs of Beluga sandstones. A. General view, showing abundant argillaceous sedimentary rock fragments (srf), which are the dominant type of framework grain. Note intergranular porosity (φ). B. Ductile deformation of argillaceous sedimentary rock fragments (srf) reduces IGV to low levels. The SRFs contain significant microporosity. C. Fissile argillaceous sedimentary rock fragments (srf) deformed between two more rigid grains. D. Quartzose siltstone rock fragment is a relatively rigid grain compared to those with higher clay content. E. Fissile argillaceous sedimentary rock fragment (shale) containing minor quartz silt grains (arrows). F. Argillaceous chert grain with several quartz veins (arrows). These grains are highly resistant to ductile grain deformation.*

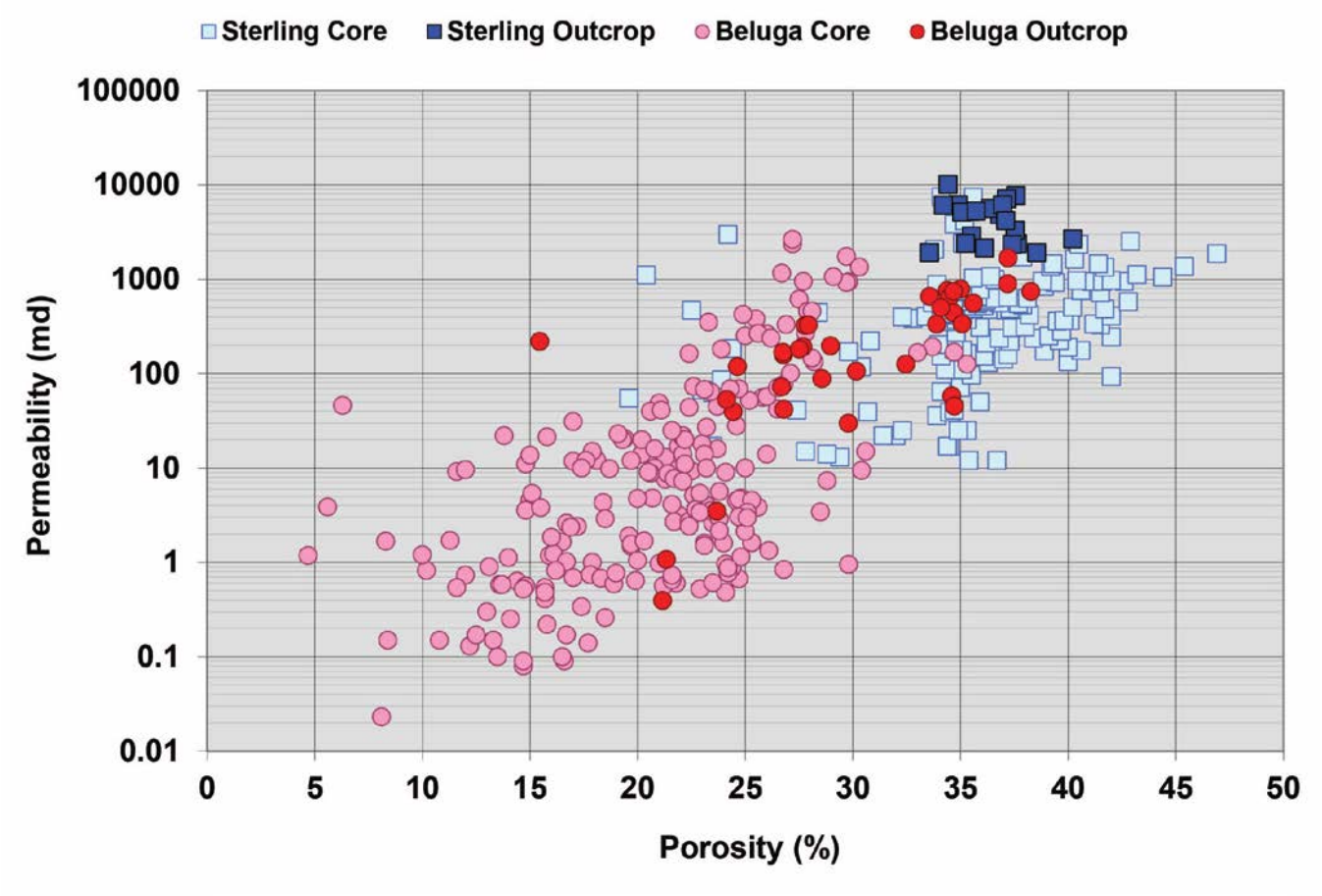

Figure 13. Porosity–permeability cross plot showing Beluga and Sterling sandstones consistently have good (φ > 15%, k > 1 md) to excellent (φ > 25%, k > 100 md) reservoir quality, which is largely a result of their young age and shallow burial. The wider range in reservoir properties for Beluga sandstones results from highly variable depositional textures.

Calderwood and Fackler (1972) correlated the Sterling Formation in the subsurface to bluff exposures along the west side of the Kenai Lowland. The mapped extent of Sterling in these bluffs, extending from Happy Valley to 4 miles (6.4 km) north of Clam Gulch, corresponds to Wolfe and others' (1966) type section for the Clamgulchian floral stage, which they regarded as Pliocene (figure 1).

Contemporaneous volcanogenic material is a significant component of the Sterling Formation, occurring as discrete tephras, primarily in coal seams, and sand-sized detrital grains of pumice and glass shards in sand bodies, particularly in the middle and upper parts (Adkison and others, 1975; Helmold and others, 2013; LePain and others, 2013). K-Ar ages on plagioclase grains and zircon fission track ages from samples collected near the base of the unit are 8.1 ± 0.7 and 7.7 ± 0.7 Ma, respectively (Turner and others, 1980). K-Ar ages from plagioclase and hornblende from a single ash sample near the top of the Sterling in outcrop near the head of Kachemak Bay are 4.2 ± 1.4 Ma and 4.7 ± 0.8 Ma, respectively. Using inorganic geochemical data and glass shard morphologies, Reinink-Smith (1995) was able to correlate tephras near the top of the exposed Sterling north-west of the head of Kachemak Bay and north of Clam Gulch. $^{40}Ar/^{39}Ar$ dates on plagioclase and hornblende grains, and volcanic glass, extracted from disrupted ash layers in coal seams from Sterling outcrops within a few miles north and south of Clam Gulch yielded ages ranging from 9.23 ± 0.97 Ma to 3.17 ± 1.58 Ma. These isotopic age dates indicate a Miocene to late Pliocene age for the formation. ARCO considered the age of the Sterling to range from middle Miocene to late Pliocene, reflecting the time-transgressive nature of the Tertiary formations in the basin (figure 4; Swenson, 2003).

Stratigraphy and Sedimentology

Bluff exposures of the Sterling Formation extend from Anchor Point northward to a few miles north of Clam Gulch, and represent nearly the entire thickness of the formation in this part of the basin, which is estimated to be around 3,000 feet (915 m). As with the Beluga near Homer, the Sterling Formation in this area is cut by numerous high-angle faults. As noted above, the contact between the two formations is gradational over several hundred feet and characterized by a gradual increase in the thickness and lateral continuity of sandstone bodies, and a corresponding decrease in the thickness of interbedded mudstones and coal seams, and decreasing coal quality (thinner coals with higher ash content; Barnes and Cobb, 1959; Calderwood and Fackler, 1972).

The Sterling Formation consists of thickly interbedded sand bodies and siltstone–claystone successions. Sand bodies in the lower part of the formation (between Anchor Point and Ninilchik) include tabular and lenticular forms up to 65 feet (19.8 m) thick, whereas sand bodies in the upper part of the unit (near Clam Gulch) tend to be tabular units up to 100 feet (30 m) thick, composed of amalgamated fluvial channel-fill deposits (figure 14a-b). Sand bodies are light tan to brown colored, friable, and commonly display an upward-fining grain size profile only in the upper few feet or so, ranging from medium to coarse sand near the base to very-fine to fine sand near the top. Sand bodies comprise lenticular and tabular beds up to 15 feet (4.5 m) thick of trough and planar cross-bedded sand and plane-parallel to wavy laminated sand (figure 15a-c); internally massive beds are also common. Cross-bed set thickness ranges from less than a foot to more than 7 feet (2 m) and tends to decrease upsection within a single sandy unit. Most sand bodies include numerous scour surfaces that extend a few feet to many tens of feet laterally (figures 14b and 15d); scour surfaces are often discontinuously lined with granule- and pebble-sized clasts, most commonly including mudstone rip-ups, coal spar, and coalified woody debris, but also including less abundant extrabasinal lithologies (figure 15c). Isolated pebble-, cobble-, and less commonly boulder-sized clasts occur widely scattered in some sand bodies and appear to "float" in a sand matrix. Light yellow to yellow-white sand-sized grains of pumice are a conspicuous detrital component in sands in the upper part of the formation near Clam Gulch, and are commonly concentrated along foreset laminae (figure 15e). Detrital pumice is abundant in sandstones at Clam Gulch and will be examined during the first beach walk. The composition of sands in the Sterling Formation are discussed below.

Finer-grained deposits up to 40 feet (12 m) thick consisting of interbedded siltstones, claystones, and dark brown lignitic coal seams separate sand bodies (figures 14a-b, 15d, and 16a). Siltstones and claystones are medium brown to dark gray and typically display massive, blocky, or platy parting in outcrop. Poorly to moderately preserved plant megafossils are present on some parting surfaces, most commonly in claystones. Locally these fine-grained lithologies appear tuffaceous and include thin beds (< 1 inch to 6 inches [2.5–15 cm] thick) of light pale yellow to brown altered tephra. Coal seams commonly include disrupted tephras. Very-fine- to fine-grained sandstones occur within siltstone and claystone successions as thin tabular beds and bedsets up to 6 feet (1.8 m) thick. Fine- to very-fine-grained sandstone fills small channels up to 15 feet thick and 80 feet wide (4.6 m thick and 24 m wide), and are widely scattered in mudstone successions. Channel-form bodies of bedded siltstone and silty claystone up to 20 feet (6 m) thick with form-concordant stratification are present locally in both the lower and upper parts of the formation.

Along the eastern basin margin, along the Fox River north of Kachemak Bay, the Sterling includes thick beds of pebble and cobble conglomerate with thin lenses of coarse-grained, pebbly sandstone. A short distance west of these outcrops, exposures along west-flowing drainages include interbedded sandstones and mudstones similar to those seen in the bluffs at Clam Gulch.

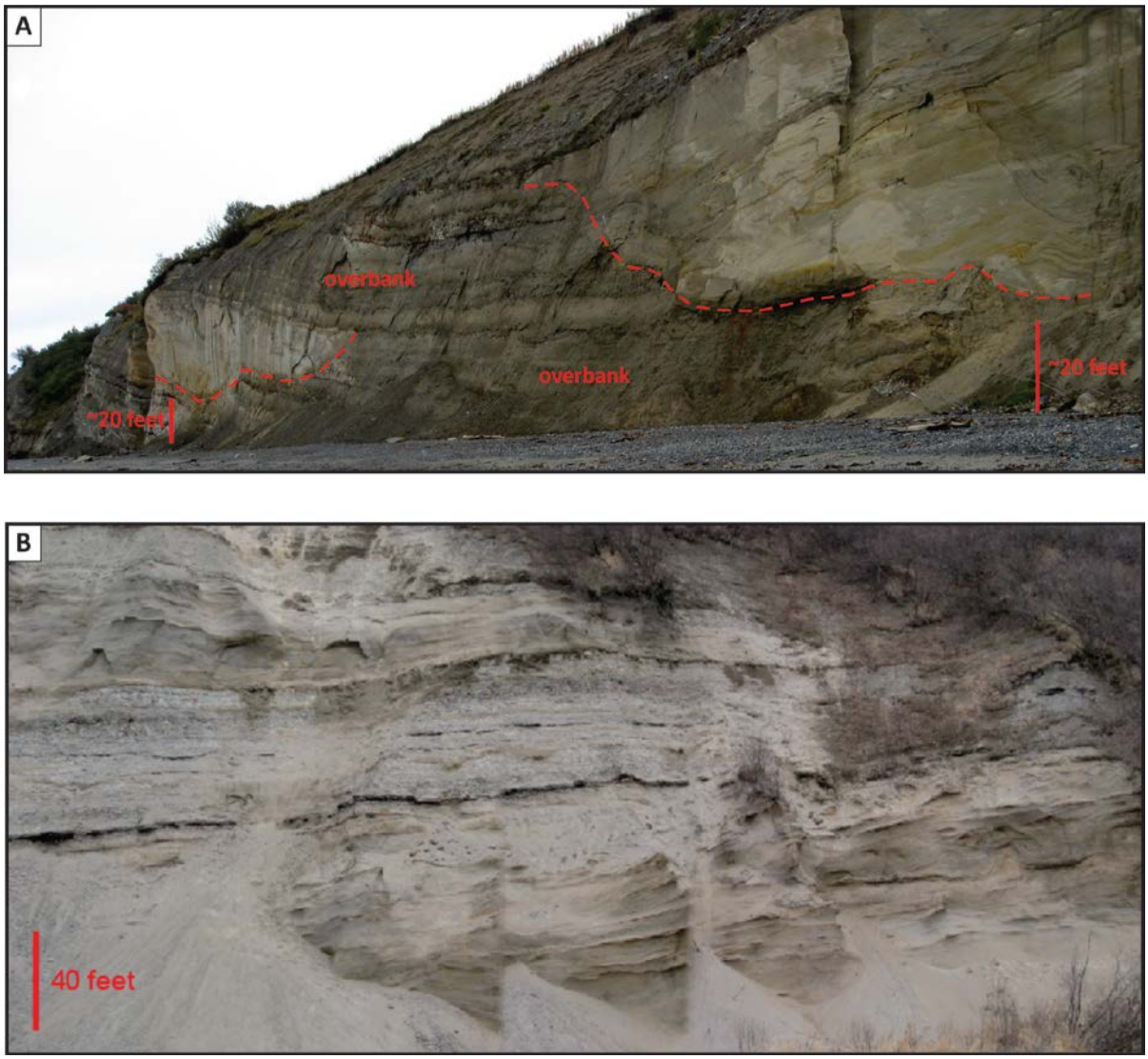

Figure 14. Photomosaic, showing stratigraphic organization of the Sterling Formation. A. Lenticular fluvial sand bodies encased in overbank mudstone a few miles north of Ninilchik. Dashed red lines mark the base to two channel-fill sand bodies. B. Sheet-like sand bodies separated by coal-bearing overbank mudstones approximately 0.5 miles north of the beach access road at Clam Gulch. Note the laterally continuous coal seam (dark band dipping gently toward the left - north) near the base of the overbank mudstone package separating two tabular sand bodies - one at the base of the exposure and the second near the top.

The gradual upsection change in sand-body geometries observed in outcrops from Anchor Point to Clam Gulch record gradual changes in fluvial style through time. In the lower part of the formation, tabular sand bodies with through-going dipping, lateral accretion surfaces suggest deposition in high-sinuousity "meandering" streams (Flores and Stricker, 1993; Mongrain, 2012; LePain and others, 2013). Thick, lenticular sand bodies with channel-form cross-sections, also in the lower part of the formation, suggest deposition in single-thread, high-sinuosity channels (anastomosing channels; LePain and others, 2013). Thick, tabular sandstone bodies recognized at Clam Gulch, with their complex facies composition and numerous internal scour surfaces, are the depositional products of a low-sinuosity, sandy, "braided" fluvial system (Flores and Stricker, 1993; Mongrain, 2012; LePain and others, 2013). While the outcrop data suggest an overall change in fluvial style through time in the Sterling, outcrop data also indicate that, at any given time, a variety of channel morphologies/ styles were likely present in a given area in the basin. Pebble and cobble conglomerates along the eastern basin margin are alluvial fan deposits shed westward from the uplifted subduction complex (Chugach terrane,

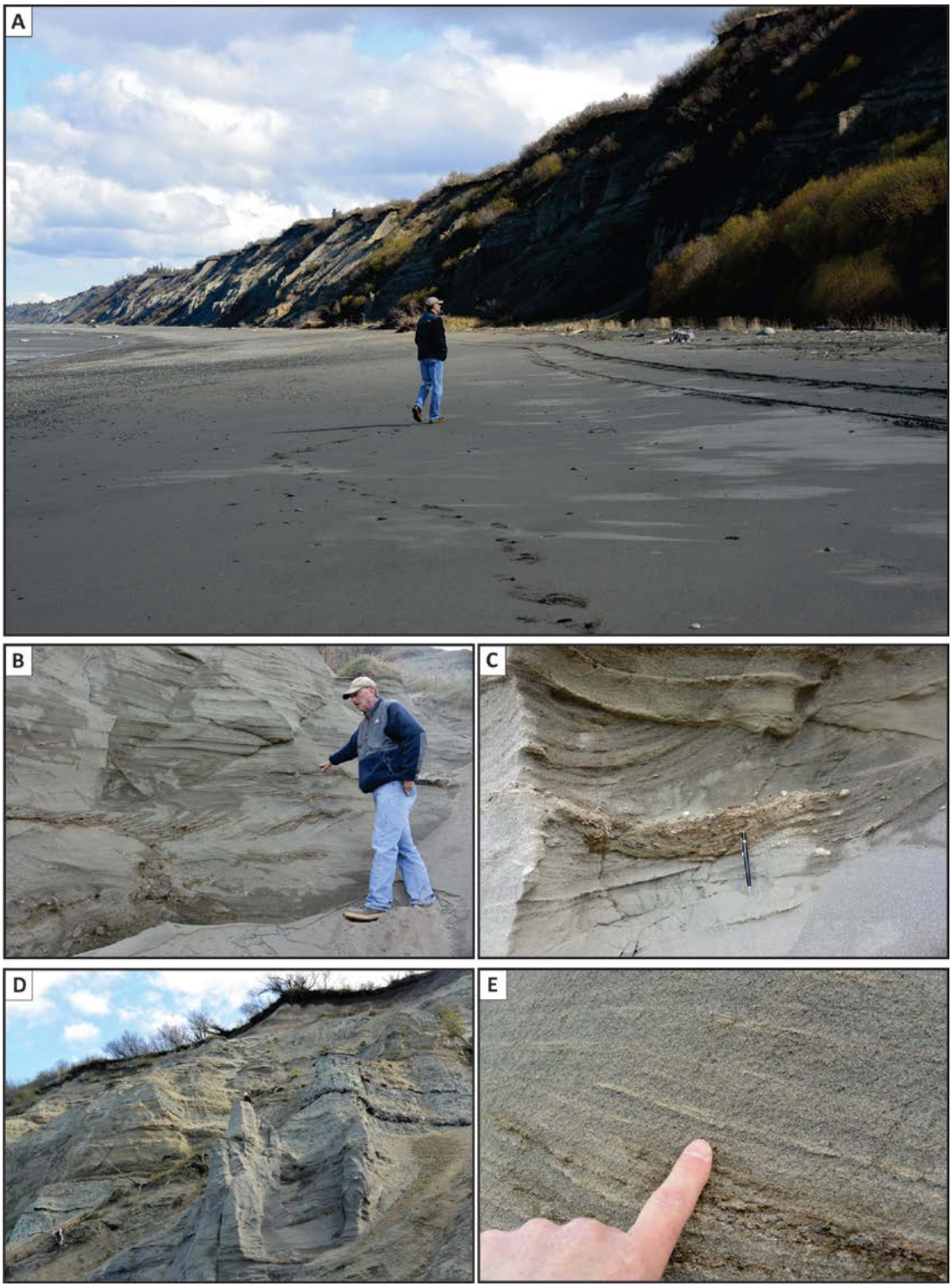

Figure 15. *A. View toward the north, showing bluff exposures of the Sterling Formation north of the beach access road at Clam Gulch. These exposures will be examined during our first beach walk. B. Close-up view, showing interbedded, cross-bedded, and horizontally laminated sand near the base of the bluff at Clam Gulch. C. Lag accumulation consisting of mudstone rip-up clasts and transported woody debris near the base of foreset laminae in cross-bedded sandstone in the same sand body shown in B. D. Convoluted bedded sand below the bald eagle near the center of the photograph. This sand body is overlain by coal-bearing overbank mudstones. E. Trough cross-bedded sandstone with sand-sized pumice fragments concentrated along selected foreset laminae. Same sand body as in B.*

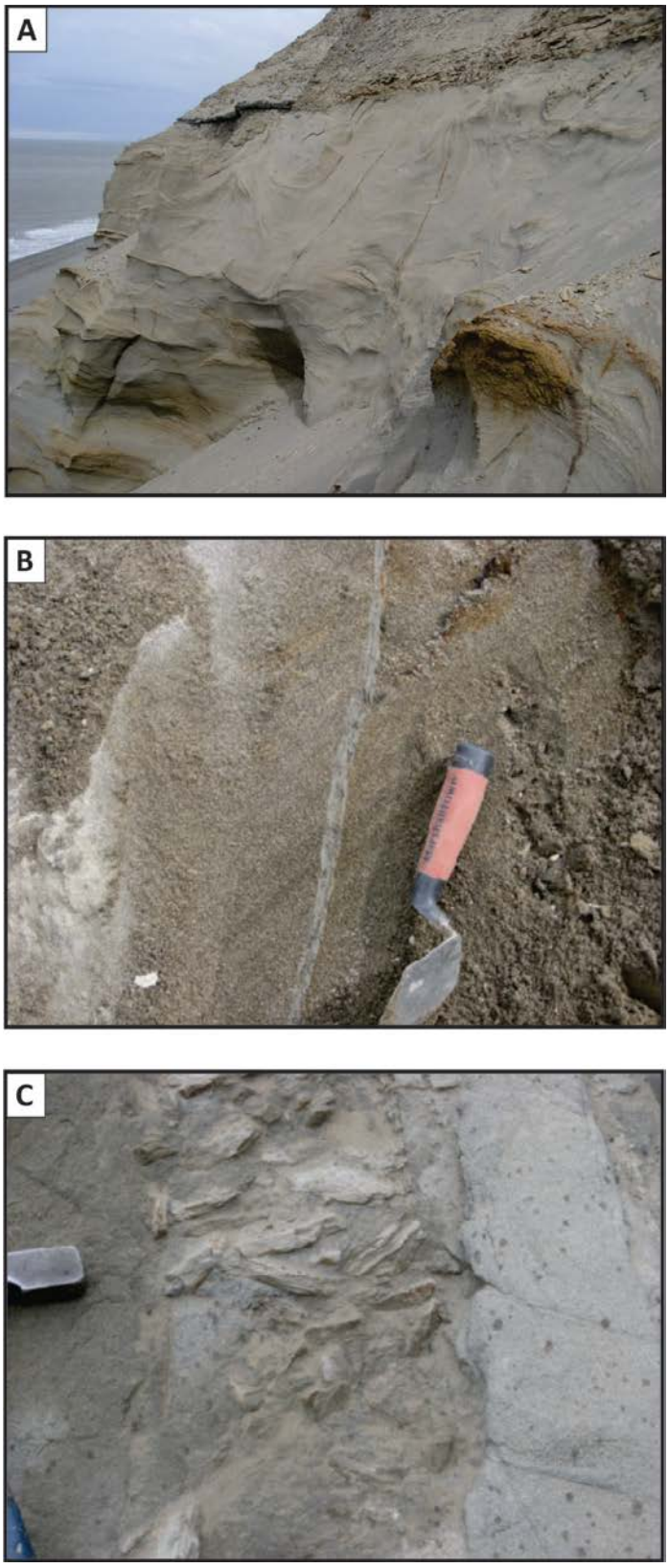

Figure 16. Photographs of deformation features in the Sterling Formation at Clam Gulch. A. Convolute bedded sandstone at the top of a sand body. B. Clay-filled dike cutting through a sand body. C. Sand breccia-filled dike near the top of a sand body.

Chugach Mountains). Recent work on the sedimentology and reservoir potential of the Sterling Formation is summarized in LePain and others (2008), LePain and others (2009), LePain and others (2013), Mongrain (2012), and Helmold and others (2013). Previous studies by Hayes and others (1976), Rawlinson (1984), and Flores and Stricker (1992) also address the sedimentology of the formation.

Soft-Sediment Deformation and Liquefaction Features—Soft-sediment deformation features are recognized throughout the unit in outcrop, but are very abundant at Clam Gulch. These features typically include disharmonic, chaotic-appearing folds that range from small-scale features isolated to a single bed to large-scale features encompassing multiple beds over thicknesses of 5 to 15 feet (1.5 to 4.5 m; figure 16a). At a few locations, soft-sediment-deformed stratified beds (for example, plane-parallel laminated, cross-bedded, etc.) grade laterally to small, irregularly-shaped masses of massive sandstone and resemble lateral changes observed in the Beluga Formation described above.

At Clam Gulch several sand bodies include clay-filled, dike-like structures up to a few inches thick that extend from the contact with underlying siltstone–claystone successions upward through the thickness of the body (figure 16b). Some dike features grade upward to funnel-shaped structures that are filled with angular pebble- to cobble-sized fragments of friable sandstone identical to the host sand body (figure 16c). The three-dimensional geometry of these features is unknown.

Soft-sediment deformation features suggestive of liquefaction, and the sediment-filled dikes are interpreted to record cyclic loading associated with large earthquakes. Clay- and sandstone breccia-filled dikes are interpreted as injectites, but their origin is poorly understood. Were they injected upward or downward? One possibility involves injection upward from a water-saturated, muddy overbank package (or packages) in the shallow subsurface, under several tens of meters of overburden, during an episode of intense earthquake-induced cyclic loading. In this scenario pore pressures increased in the source mudstone package until a threshold was exceeded and a sediment–water slurry was injected into the overlying column of sediment (natural hydraulic fracturing).

The abundance of sand-sized pumice fragments, plagioclase and hornblende grains, and pristine glass shards in sands from the upper Sterling at Clam Gulch (see next section) suggest deposition during a period of increased volcanic activity in the nearby arc. Air-fall tuffs and pyroclastic flows deposited on the flanks of active volcanoes are easily eroded during volcano–hydrologic events (in the sense of Smith and Lowe, 1991) and would have resulted in large volumes of sediment being supplied to streams over relatively short periods of time. The capacity of many streams to move sediment could easily have been exceeded during the decades and centuries following significant volcanic eruptions. The net result would have been rapid deposition of thick beds of sand. These would have been metastable and particularly susceptible to soft-sediment deformation. An earthquake or subsequent flood event could easily trigger soft-sediment deformation.

Composition and Reservoir Quality of Sandstones in the Sterling Formation

Sandstones of the upper Miocene and Pliocene Sterling Formation vary in composition throughout the stratigraphic section. The transition in provenance from the middle Beluga through the upper Sterling Formations is discussed at length in a following section. In general, Sterling sandstones are volcanogenic with an average modal composition of $Q_{20}F_{20}L_{60}$, $Q_{m8}F_{20}L_{t72}$, $Q_{m28}P_{64}K_{8}$, $Q_{p18}L_{vm65}L_{sm17}$ (figure 10) and a P/F ratio of 0.89. The average grain size is 0.31 mm (lower medium) with an average Folk sorting of 0.55 (moderate; figure 11b). Felsic and intermediate VRFs are the dominant type of framework grain (figure 17a) and show relatively little alteration. Pumiceous (figure 17b-c) and vitrophyric (figure 17d-e) grains are common, as are hornblende and basaltic hornblende, which are relatively fresh, showing little alteration or dissolution (figure 17f). Twinned plagioclase is the dominant feldspar and is largely unaltered; K-feldspar is a minor component. Monocrystalline quartz is a minor framework component and is probably of volcanic origin as indicated by its water-clear,

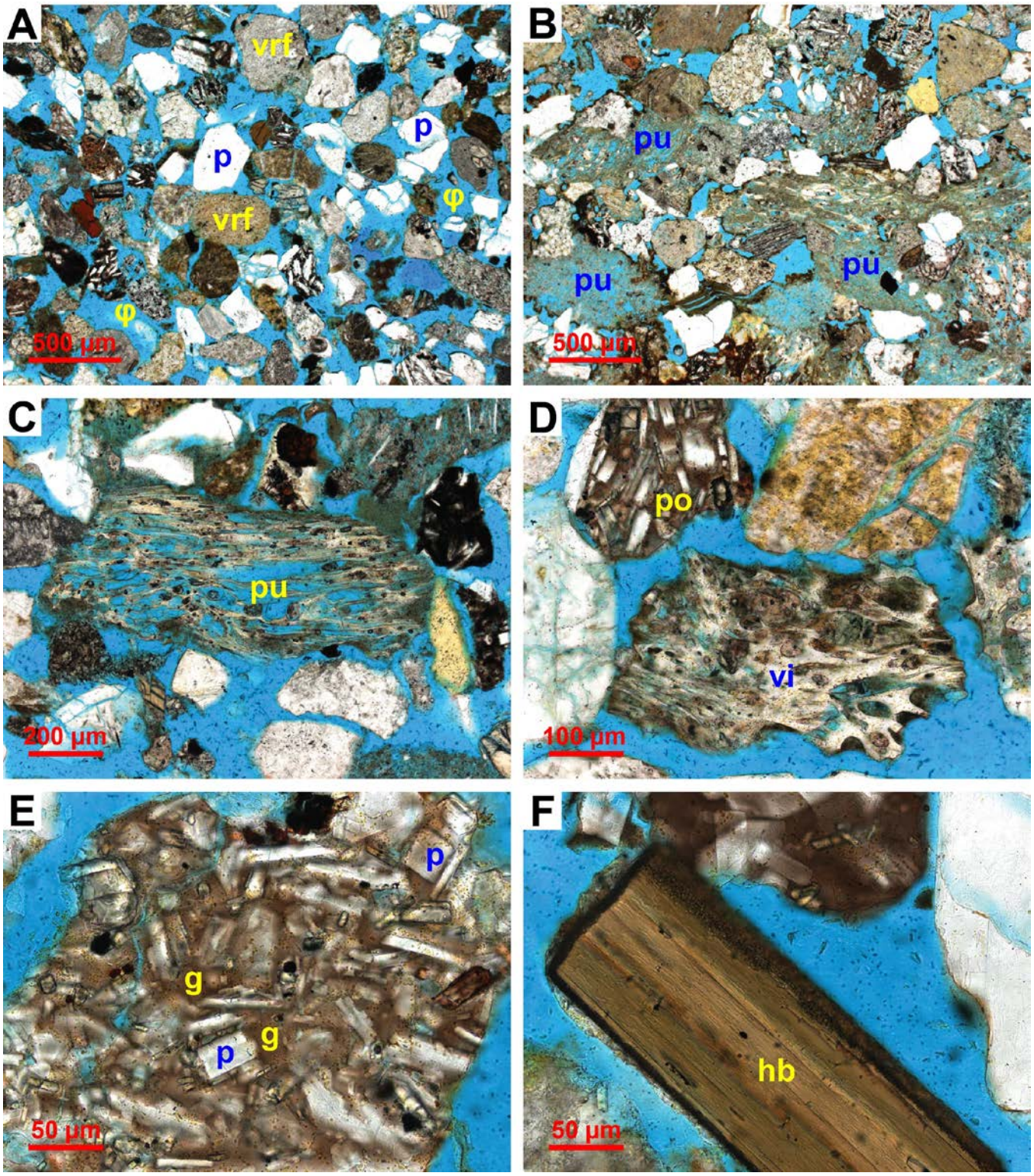

Figure 17. *Photomicrographs of Sterling sandstones. A. General view, showing abundant volcanic rock fragments (vrf), plagioclase (p), and heavy minerals. Excellent reservoir quality results from extensive intergranular porosity (φ). B. Abundant pumice grains (pu) with significant microporosity due to vesicular texture. C. Pumice fragment (pu) consisting largely of glass with vesicular texture. D. Volcanic rock fragments with porphyritic (po) and vitrophyric (vi) textures are the dominant type of framework grain. E. Porphyritic volcanic rock fragment with glassy groundmass (g) and plagioclase phenocrysts (p). F. Pristine detrital hornblende grain (hb) suggests some volcanic detritus is syndepositional in origin.*

relatively unstrained character and occasional straight sides. The IGV is slightly more than 30 percent, indicating that the rocks have not undergone significant compaction. Cements average less than 1 percent of the bulk rock, indicating negligible porosity loss through cementation. As expected from its young age, relatively shallow burial, lack of compaction or cementation, Sterling sandstones have good to very good reservoir quality with porosities in excess of 30 percent and permeabilities of several darcies (figure 13) and comprise many of the shallow gas reservoirs in the inlet.

Sterling Formation grain composition suggests a magmatic arc provenance. The volcanogenic composition and pristine appearance of most detrital grains suggests much sand was derived from only slightly older to coeval arc-related volcanic deposits. In particular, detrital hornblende is fresh and unaltered (figure 17f) and is in stark contrast to hornblendes in older sandstones (such as the West Foreland Formation) that are largely altered and partially dissolved.

Beluga–Sterling Provenance Transition

Modal analyses of the Sterling and Beluga sandstones (Helmold and others, 2013) suggest there is an evolution in provenance of the sandstones through time. There appears to be a transition from middle Beluga sandstones with a solely argillaceous composition, through upper Beluga and lower Sterling sandstones with a mixed mineralogy, to upper Sterling sandstones with a significant volcaniclastic component (figure 18a). Sandstones from the middle portion of the Beluga Formation collected at Fritz Creek (figure 18b) consist almost exclusively of argillaceous sedimentary and metasedimentary rock fragments with only minor quartz and virtually no volcanic detritus (figure 18a). They are believed to be representative of Beluga sandstones from the lower and middle portions of the formation. This detritus is interpreted to have been derived largely from the subduction complex and/or sources in the Alaska Range orogen represented by the Kahiltna assemblage north of Cook Inlet basin.

Sandstones from the upper Beluga Formation collected at Bidarka Creek (figure 18b) have a mixed mineralogy consisting of argillaceous SRFs/MRFs, volcanic rock fragments, plagioclase and amphiboles. Likewise, sandstones from the lower Sterling Formation collected at Falls Creek (figure 18b) consist of a similar mixture of argillaceous SRFs/MRFs and VRF-plagioclase detritus. These sandstones are interpreted to have been derived from multiple sources including the subduction complex, Kahiltna assemblage, Alaska Range orogen, and recycled older Cenozoic formations in Matanuska Valley.

Sandstones from the upper portion of the Sterling Formation collected at Clam Gulch (figure 18b) are very volcanogenic (figure 18a) with abundant VRFs, very high P/F ratio, significant quantity of detrital amphiboles, and common pumice and unaltered glass fragments probably of pyroclastic origin. These sediments are interpreted to have been sourced from a mixture of older, undissected segments of the Alaska–Aleutian Range volcanic arc and penecontemporaneous volcanic edifices ejecting pumiceous material, with possible additional contributions from the Alaska Range orogen and recycled strata from the collapsed Matanuska Valley segment of the forearc basin (figure 18).

In summary, during the middle Miocene when the lower Beluga Formation was deposited, detritus was derived almost exclusively from source terranes composed dominantly of shale and argillite. The Chugach accretionary complex on the east side of the basin is assumed to be the dominant source of the argillaceous material but the Kahiltna assemblage north of Cook Inlet is a possible secondary source. Starting around 8–10 ma (middle–upper Miocene) an additional sediment source gradually became more prominent on the west side of the basin in the Alaska–Aleutian Range volcanic arc complex, yielding both epibasinal volcanic and coeval pyroclastic material. Through time an increasing proportion of sediment was derived from this western volcanic provenance. The transition culminated around 4 Ma (middle Pliocene) when the eastern sediment source was shut off and detritus was solely derived from the Aleutian–Alaska Range volcanic arc and collisional sources to the

north and west of the basin. This discussion assumes the argillaceous sedimentary and metasedimentary detritus was derived largely from the Chugach accretionary complex, with minor northerly input from the Kahiltna complex. While this is the simplest interpretation, additional work is needed to ascertain its validity.

A

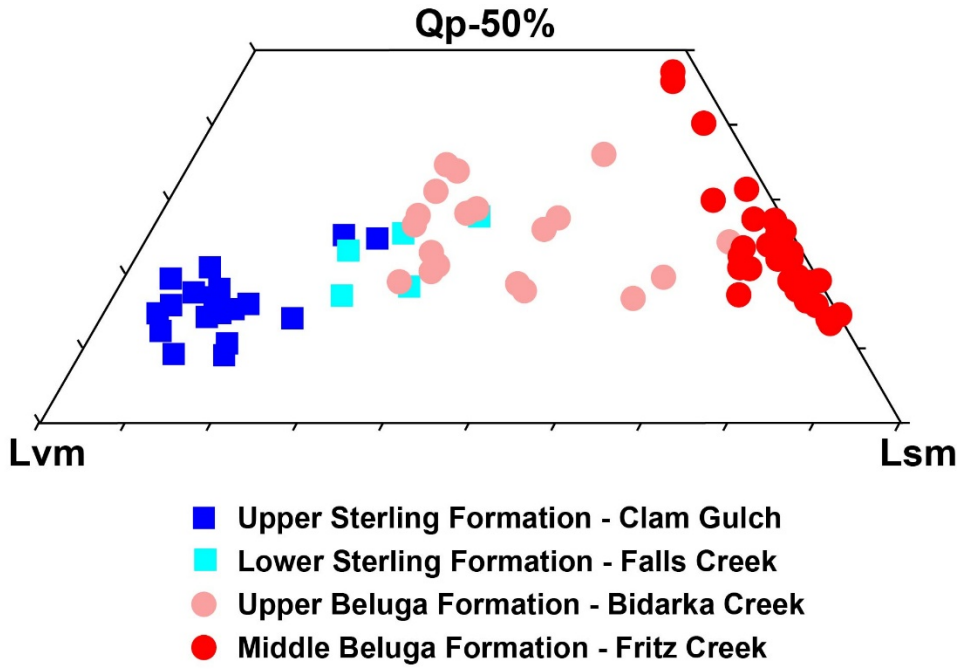

B

Ma	Formation	Location
4	Upper Sterling	Clam Gulch
6		
8	Lower Sterling	Falls Creek
	Upper Beluga ?	Bluff Point
10	Upper Beluga	Bidarka Creek
12		
14	Middle Beluga	Fritz Creek

Figure 18. Diagrams documenting the Beluga–Sterling provenance transition. A. Lower half of a QpLvmLvs diagram, showing the change in composition of the Beluga and Sterling sandstones through time; see text for discussion. B. Absolute and relative ages of Beluga and Sterling sandstones from outcrops where samples were collected.

STRUCTURAL STYLE AND TIMING OF DEFORMATION IN BASIN

Cook Inlet basin is elongated in a northeasterly direction and major folds in the basin are arranged in an en echelon pattern with axes trending north–northeast, slightly oblique to the basin axis (figure 2). This pattern is evident on maps showing the locations and plan-view shapes of producing oil and gas fields, which are all located along the crests of these structures (Kirschner and Lyon, 1973; Haeussler and others, 2000). Fold axes are gradually deflected eastward as they approach the Castle Mountain fault zone, which is consistent with right-lateral motion documented for the fault (Kirschner and Lyon, 1973; Haeussler and others, 2000). Fold axes approach the Bruin Bay fault zone at a very low angle or are parallel to the fault.

Haeussler and others (2000) analyzed several fault-propagation folds in the upper Cook Inlet segment using two-dimensional seismic reflection data, published cross-sections, and structure contour maps for selected fields. They noted that folds are located throughout the basin, but that those on the west side record more shortening (figure 3). Most folds are asymmetric, doubly plunging, and many include high-angle transverse faults (see basin overview poster; Kirschner and Lyon, 1973, their figure 18; Haeussler and others, 2000, their figure 4). Folds along the west side of the basin are located along an up-to-west step in Mesozoic basement, while folds along the east side are located along a down-to-west basement step. The modeled fault-propagation folds on the west side of the basin involve Mesozoic basement, and many have opposing senses of vergence with a main thrust fault coring the structure and a backthrust that intersects it at depth (Middle Ground Shoal is a good example). These transpressional structures are the result of dextral oblique motion along the Castle Mountain and Bruin Bay fault zones (Haeussler and others, 2000). However, new geologic mapping along the northwestern margin of the basin (Gillis and others, in preparation) has identified transtensional structures deforming Eocene strata of the West Foreland Formation. In the nearby subsurface, well log and seismic interpretation defines a thick wedge of West Foreland and other Paleogene strata in the hanging wall of the Bruin Bay fault/Moquawkie structure that indicates Paleogene transtensional structures have been inverted by later transpression, at least locally.

Haeussler and others (2000) noted that isopachs of the younger Tyonek Formation were relatively uniform over fold structures, the Beluga thins slightly over fold crests, and the combined Sterling and Quaternary sediments either thin over crests or are eroded off the crests of fold structures. These observations suggest that the latest phase of deformation began no earlier than late Miocene and continued into the Quaternary, and active seismicity associated with many structures indicates that deformation continues to the present day (Haeussler and others, 2000). The earlier transtensional phase overlaps with latest Paleocene subduction of a spreading ridge, subsequent rollback of the subducting slab, and middle Eocene re-initiation of arc magmatism (Bradley, and others, 2000; Todd and others, 2014). The latest phase of deformation is linked to collision of the Yakutat block with Alaska starting in the Miocene (Plafker and others, 1994).

PETROLEUM GEOLOGY OF COOK INLET BASIN

Cook Inlet basin includes three known petroleum systems (Magoon, 1994): 1. The Tuxedni–Kaguyak system, which includes oil generated from Middle Jurassic source rocks and reservoired in Campanian–Maastrichtian sandstones, but has not been produced commerically; 2. The Tuxedni–Hemlock system, which includes oil generated from Middle Jurassic source rocks and reservoired in the Paleogene and Neogene nonmarine sandstones of the West Foreland Formation, Hemlock Conglomerate, and Tyonek Formations; and 3. The Beluga–Sterling system, which includes microbial gas generated from Tertiary coal seams and reservoired in sandstones of the Beluga and Sterling Formations. All of the oil produced in the basin comes from the Tuxedni–Hemlock system and most of the gas is produced from the Beluga–Sterling system. As of the end of 2010, more than 1.3 billion barrels of oil and about 8 trillion cubic feet of gas have been produced from these two petroleum systems (Hite and Stone, 2013; LePain and others, 2013).

All of the oil and gas produced in the basin comes from conventional reservoirs in structural traps on anticlines and faulted anticlines with four-way closure (figures 2 and 5). Timing of oil generation in the basin is poorly constrained. Recent modeling suggests that peak oil generation probably started about 15 Ma between Middle Ground Shoal and Swanson River, where the Tertiary succession is thickest, and peak oil generation along the eastern and southern margins of the basin has probably not yet begun (Lillis and Stanley, 2011). As stated previously, seismic data indicate that fold structures in upper Cook Inlet are relatively young features with uplift mostly occurring from Pliocene to the present day (Haeussler and others, 2000). Uplift of these structures resulted in desorption of gas in Neogene coal seams and subsequent migration into conventional sandstone reservoirs in the Beluga and Sterling Formations. Faults coring these structures represent important migration pathways for oil.

Oils produced from Cook Inlet fields generally have an API oil gravity of 34°, but oil gravity ranges from 18 to 53° API, low sulfur content (about 0.1%), and gas:oil ratios of about 600 cubic feet of gas per barrel of oil (Magoon and Kirschner, 1990; Magoon, 1994; LePain and others, 2013). Organic geochemical data, including carbon isotopes and biomarkers, indicate that the principal source rocks for oil and associated gas in the basin are organic-rich marine shales of the Middle Jurassic Tuxedni Group (Magoon and Anders, 1992; Magoon, 1994, LePain and others, 2013). Nonassociated microbial gas, derived largely from Tertiary coal seams, accounts for about 92 percent of Cook Inlet gas production (Thomas and others, 2004).

In 2011 the U.S. Geological Survey assessed the undiscovered, technically recoverable oil and gas resources in Cook Inlet basin using a geology-based assessment methodology (USGS, 2011). The mean volume of undiscovered, technically recoverable conventional oil, natural gas liquids, and gas in the basin is estimated at 599 MMBO, 37 MMBNGL, and 13.7 TCF, respectively. The mean volume of undiscovered, technically recoverable unconventional natural gas liquids and gas in the basin is estimated at 9 MMNGL and 5.1 TCF, respectively.

DESCRIPTION OF FIELD TRIP STOPS

The Miocene and Pliocene stratigraphy visible in bluff exposures rimming the western and southern sides of the Kenai Lowland is easily accessible. These strata have not been deeply buried and subjected to compaction and extensive burial diagenesis. Consequently they are weakly to moderately consolidated and weakly cemented. Well-cemented (siderite) beds and siderite concretions are present locally. Because of the weakly cemented nature of the stratigraphy, the bluffs are unstable and prone to spontaneous mass movements. This is especially true during and immediately following major rain events. Exercise extreme caution when approaching the base of the bluffs. Be sure to look up the bluff and make sure no overhanging ledges or vegetation are present. The safest situation is when the bluff slopes back from the beach.

Clam Gulch

The first beach walk will take place at Clam Gulch, a location a short distance south of Soldotna that is popular for set-net fishermen and the general public for digging razor clams at low tide (figure 19a). Bald eagles are abundant in this area and can often be seen perched on the bluffs. The group will walk from the campground down a short, steep beach access road. Once on the beach the group will turn right and walk north along the base of the bluffs. Low tide (1.4 ft) at Cape Kasilof (a short distance north of Clam Gulch) on June 16 is 8:32 AM and high tide (16.7 ft) is 2:52 PM, so the tide will be coming in during the group's visit (table 1). Good exposures of the Pliocene Sterling Formation are visible in the bluffs both north and south of the beach access road. Thick tabular sand bodies separated by flood basin mudstones dip gently toward the north (figures 20 and 21). Approximately 200 feet (61 m) of Sterling section is visible in the bluffs between the access road and north end of the beach walk (~0.5 miles [0.8 km] from the access road).

The bluff exposures viewed during this beach walk provide a nice view of the Pliocene alluvial depositional system (Sterling Formation) in upper Cook Inlet basin. The exposed sand bodies represent important analogs

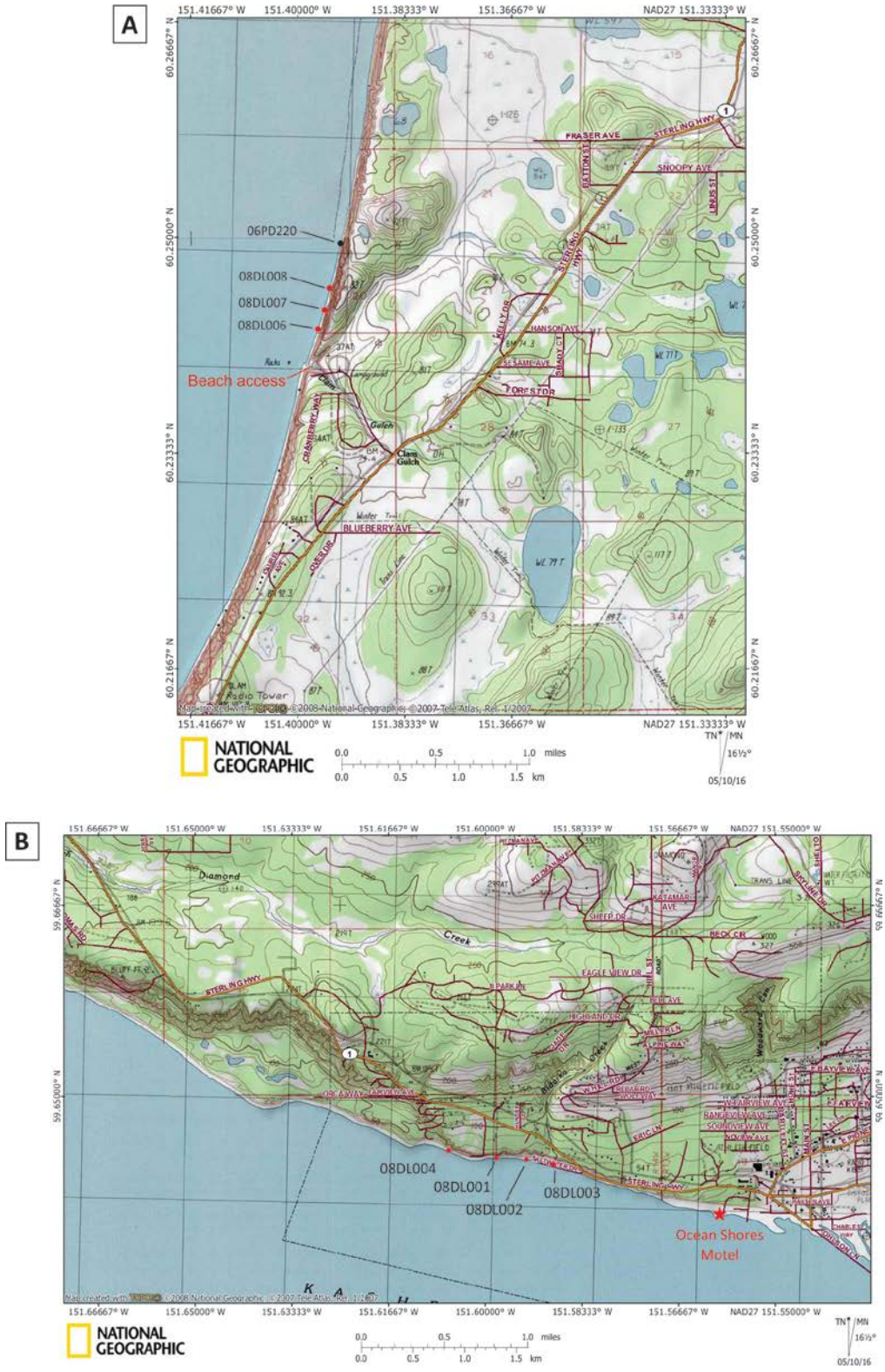

Figure 19. A. Topographic map of the Clam Gulch vicinity, showing the location of the first beach walk. Red dots mark the locations of measured stratigraphic sections shown in figures 20 and 21. Measured section 06PD220 (black dot) is not included in figures 20 and 21, as it beyond walking distance from the beach access road given the available time, but it includes a suite of facies similar to those seen in the other measured sections. B. Topographic map, showing the beach and bluffs west–northwest of Homer. Red dots mark the locations of measured stratigraphic sections shown in figures 22 and 23.

for producing gas reservoirs in the subsurface. Sandstones are weakly cemented and display an interesting array of sedimentary structures, including trough cross-bedding, plane-parallel lamination, convolute bedding, and scour surfaces discontinuously lined with a variety of pebble-sized clasts (figure 21). Most sand bodies appear tabular, but occasional visible thinning of some suggest broadly lenticular geometries may also be present. Some sand bodies include liquefaction features and thin, clay-filled dikes (figures 16a-c and 21). Sands include a significant volcanogenic component, including pumice fragments, pristine glass shards, and unaltered hornblende and plagioclase crystals (figure 17a-f). The pristine character of this material strongly suggests volcanism was contemporaneous with deposition of this part of the Sterling. Mudstones include massive and finely laminated varieties, and the former typically displays blocky weathering character. Poorly to moderately preserved plant fossils (leaf impressions) are common on mudstone parting surfaces. Thin (up to 3.5 feet [≤ 1.1 m]) seams of lignitic coal are common in mudstone successions, but less abundant than in the underlying Beluga Formation.

Some questions to consider while examining this succession:

1. Do you agree with our interpretation that these sand bodies record deposition in low-sinuosity, sandy, braided rivers?
2. Was sediment supply low or high?
3. What are possible origins of the convolute bedding in the sands?
4. How could the clay-filled dikes have formed?
5. How would you expect contemporaneous volcanic eruptions in the nearby arc to affect fluvial depositional systems in the forearc basin?
6. Has this succession been deeply buried?
7. How would the volcanogenic composition of the sand influence reservoir quality at shallow burial depths (less than 5,000 feet [<1,500 m])? How about at a depth of 15,000 feet (~4,600 m)?

Bluff Point Overlook

On our way into Homer the bus will stop ***very briefly*** (15 minutes) at the Bluff Point Overlook to use the rest-rooms and view the Bluff Point landslide. The overlook is above the headwall of the landslide, and the slide mass is clearly visible to the south and southwest of the overlook parking area. Reger (1979) provides a description of the slide mass and a discussion of its likely origin. The description that follows is taken from his work.

The Bluff Point landslide is the largest slope failure feature along the southern shore of the Kenai Lowland. In this area the bluffs rise nearly 750 feet (230 m) from the shore. The headwall has an irregular shape, is 328 to 705 feet (100–215 m) high, and extends 5.5 km in a northwest-southeast direction. The landslide mass extends seaward from the headwall 0.56 miles (0.9 km) to the shore of Kachemak Bay. Nautical charts indicate the slide mass continues offshore an additional 0.25–0.31 miles (0.4–0.5 km). The slide mass consists of a thin veneer of Pleistocene till over weakly to moderately consolidated, middle to late Miocene sandstones, mudstones, and coals of the Beluga Formation. The surface of the landslide mass is up to 295 feet (90 m) above sea level and consists of a series of sub-parallel ridges with up to 197 feet (60 m) of local relief. Some low-lying areas are occupied by ponds. Slide deposits dip 25–30° toward the north and northeast, whereas the undisturbed Beluga Formation dips 3–5° south. The composition of landslide deposits indicate the landslide resulted from failure of the weakly to moderately consolidated Beluga Formation.

Reger (1979) states the cause of the landslide is unknown, but was probably due to the loss of support when the late Wisconsinan glacier withdrew from this location. Unpublished radiocarbon dates indicate the land-slide occurred approximately 2,250 calendar years ago (Reger, unpublished data).

The second beach walk will take place southeast of the Bluff Point landslide.

Homer

The second beach walk will take place in Homer to view exposures of the late Miocene Beluga Formation (figure 19b). The group will leave the bus at the Ocean Shores Motel, descend a steep dirt path to the beach, and head northwest along the base of the bluffs. High tide (14.0 ft) at Homer is 1:19 PM (table 1). Given that the tide will be starting to ebb at the start of this beach walk and that the high tide is predicted to be only 14 feet above mean low water (spring tides can exceed 21 feet), we should not have trouble walking along the base of the bluffs at the height of the flood tide. Approximately 200 feet (61 m) of Beluga section is exposed in the bluffs immediately above beach level. As the bluffs rise considerably higher than this, more section is exposed higher up the bluff.

The bluff exposures viewed during this beach walk provide a nice view of late Miocene depositional systems in upper Cook Inlet basin (figures 22 and 23). Sand bodies and coal seams in the bluffs are important analogs for producing gas reservoirs and source rocks for microbial gas in the subsurface. Exposures include thick, coal-bearing mudstone packages alternating with thick, broadly lenticular sand bodies (figures 7b, 8a, 22, and 23). Sand bodies include a variety of sedimentary structures, including trough cross-bedding, plane-parallel lamination, and ripple cross-lamination (figures 8 and 23). Massive sands are also common. The "Shellenbaum sand" is a brisk 45-minute walk west from the Ocean Shores Motel and includes all of the above sedimentary structures and several interpreted liquefaction features (figure 23). A bedding plane exposure in this sand includes a very nice example of rib-and-furrow structure (horizontal cut through trough cross-laminae; Pettijohn and Potter, 1964). Given time constraints, it may not be possible to see the "Shellenbaum sand" on this field trip. Sandstones in the Beluga include a significant percentage of detrital argillite fragments and interstitial clays.

Some questions to ponder while examining this succession:

1. Do you agree with our interpretation that these sand bodies record deposition in low-sinuosity, sandy, braided rivers?
2. What are possible origins of the convolute bedding in the sands?
3. Do you agree with our interpretation that localized massive sands record liquefaction?
4. How does sandstone composition differ from sandstones at Clam Gulch?
5. Has this succession been deeply buried?
6. How would the high percentage of detrital argillite influence reservoir quality at shallow burial depths (< 5,000 feet [~1,500 m])? How about at a depth of 15,000 feet (~4,600 m)?

Following the second beach walk the group will re-board the motor coach for the return trip to Girdwood for dinner. We will stop briefly in Soldotna to use restrooms at Fred Meyer.

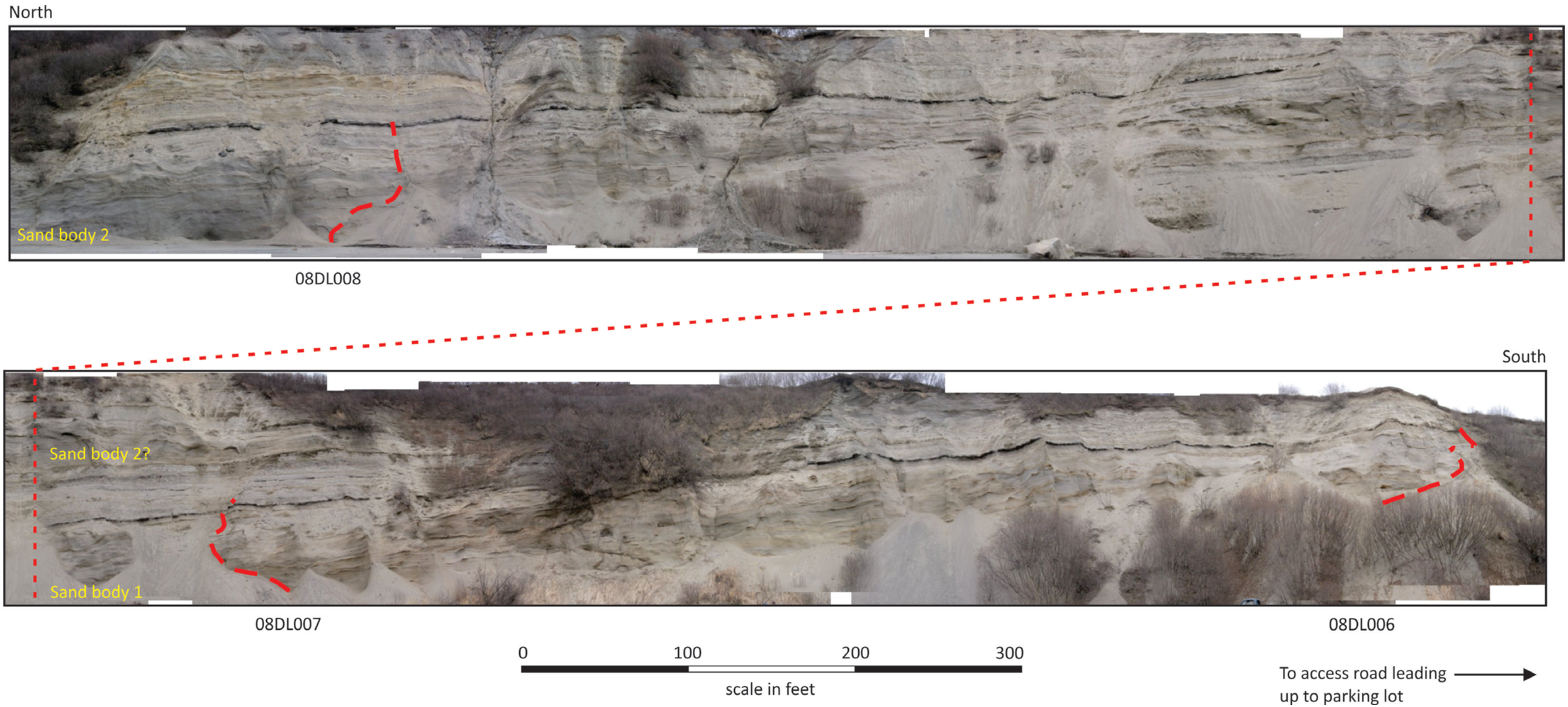

Figure 20. *Photomosaic, showing approximately 1,900 feet of bluff exposure north of Clam Gulch. Dashed red lines show locations of measured stratigraphic sections shown in figure 21.*

Key Points

- Near top of Sterling Formation
- Pumiceous sandstone reflects significant contribution from arc
- Mostly tabular sand body geometries
- Convolute bedding and fluid escape features suggest liquefaction
- Origin of convolute bedding and liquefaction features - seismogenic?
- Origin of clay-filled and breccia-filled dikes? Seismogenic?
- Fluid flow implications of clay-filled dikes - reservoir baffles

08DL008,
N60.24392 W151.39618

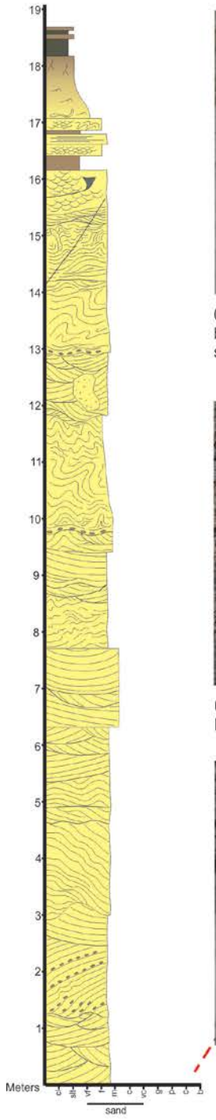

08DL008 - Small-scale trough cross-bedding at 16 m. Note pumice-rich foresets.

08DL008 - Pumice fragments in cross-bedded sand

08DL008 - Stacked sets of trough cross-strata between 0 and 4 m

08DL007
N60.24392 W151.39618

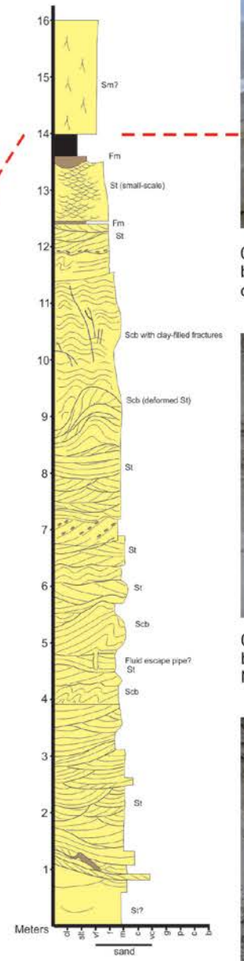

08DL007 - 12 to 13m - Convolute bedded sand with deformed trough cross-beds between 12 and 13 m

08DL007 - 1 to 3m - Trough cross-bedded sandstone between 1 and 3 m. Note pumice-rich foreset laminae.

08DL007 - Massive sand at 0 m

08DL006
N60.24232 W151.39662

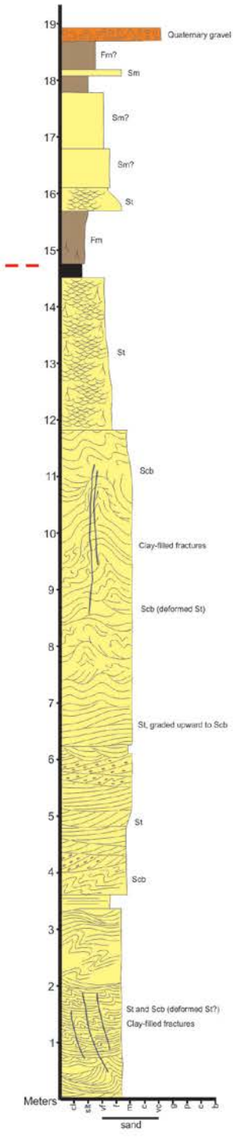

08DL006 - Breccia-filled pipe near top of sand body

08DL006 - Fluid escape pipe at 14.2 m

08DL006 - Trough cross-bedded sand-stone between 7 and 10 m

Figure 21. *Three measured stratigraphic sections through part of the Sterling Formation exposed in the bluffs north of Clam Gulch. Measured section locations are shown in figures 19 and 20. Datum for latitude and longitude is NAD27 Alaska. Photographs show selected stratigraphic features in each measured section.*

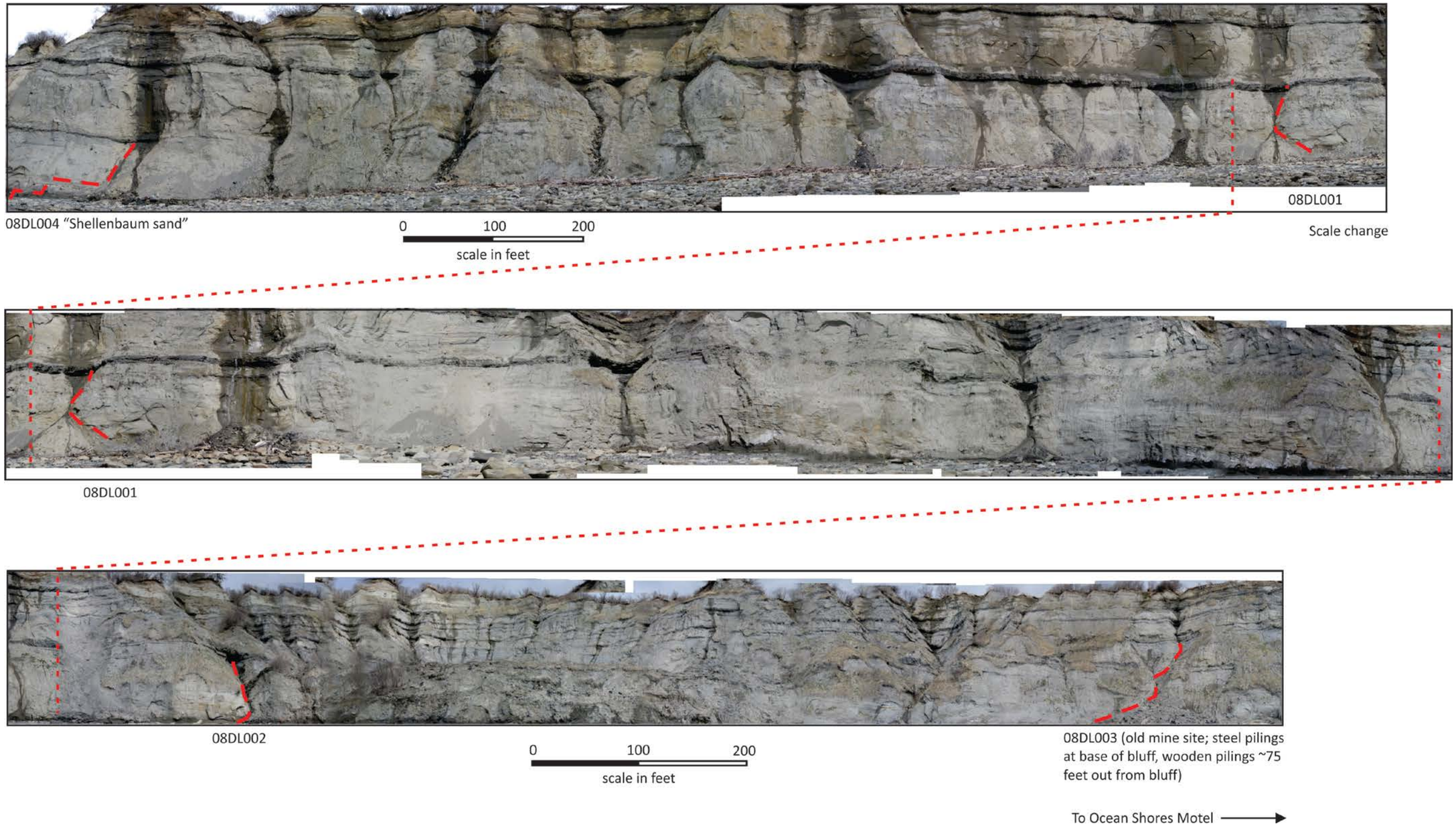

Figure 22. *Photomosaic, showing approximately 5,000 feet of bluff exposure in the upper Beluga Formation near Bidarka Creek, west–northwest of Homer. Long-dashed red lines show locations of measured stratigraphic sections shown in figure 23. Short-dashed red lines are tie lines for photomosaic segments.*

Key Points

- Near top of the Beluga Fm.
- Sand body continuity transitional between lenticular sands in lower Beluga and tabular sands in upper Sterling
- Sands are clayey and detrital grains are largely argillaceous rock fragments and quartz, but pumice is locally conspicuous
- Convolute bedding is locally prominent - as prominent as in Sterling???
- Seismogenic trigger or inherent to fluvial system?

08DL004
"Shellenbaum sand"

N59.64523 W151.60587

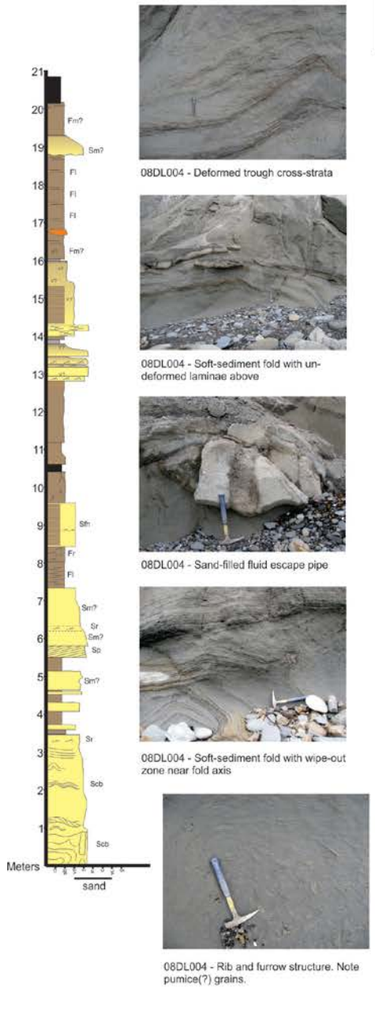

08DL004 - Deformed trough cross-strata

08DL004 - Soft-sediment fold with un-deformed laminae above

08DL004 - Sand-filled fluid escape pipe

08DL004 - Soft-sediment fold with wipe-out zone near fold axis

08DL004 - Rib and furrow structure. Note pumice(?) grains.

08DL001

N59.64457 W151.59853

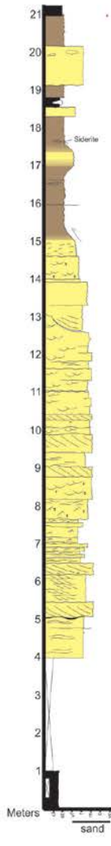


08DL001 - Argillaceous siltstone from 20 m to coal immediately above section


08DL001 - Planar-tangential foresets at 5.2 m


08DL001 - Interval between 4 to ~10 m. Note deformed Sh beds.


08DL001 - Coal at 0 m

08DL002

N59.6448 W151.59385

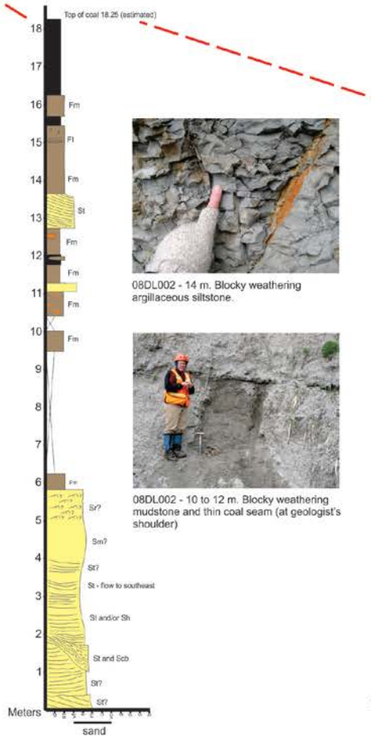

08DL002 - 14 m. Blocky weathering argillaceous siltstone.

08DL002 - 10 to 12 m. Blocky weathering mudstone and thin coal seam (at geologist's shoulder)

08DL003

N59.64458 W151.5908

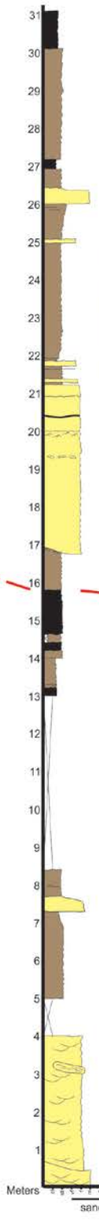


08DL003 - View up the bluff showing the interval between 20 and 30 m

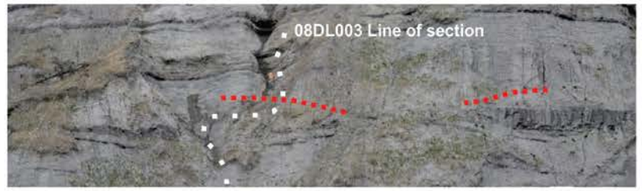

Photopan showing lateral facies relations at the level of the thick coal at 15 m in 08DL003. Sand body cuts out coal. Same coal as at 18 m in 08DL002.


08DL005 - Splay sand sheet at 7.3 m


08DL005 - Rhizoliths at 2.2 m


08DL003 - Trough cross-bedded sandstone with pumice-rich foreset laminae at 1 m


08DL003 - Trough cross-bedded sandstone at 2 m

08DL005

N59.64452 W151.58883

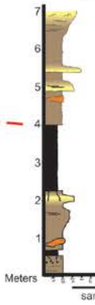


08DL005 - Coal seam at 2.3 m

Figure 23. Five measured stratigraphic sections through part of the Beluga Formation exposed in the bluffs west–northwest of Homer. Measured section locations are shown in figures 19 and 22. Dashed red line correlates the thick coal seam in the eastern four sections. Photographs show selected stratigraphic features in each section.

REFERENCES CITED

Adkison, W.L., Kelley, J.S., and Newman, K.R., 1975, Lithology and palynology of the Beluga and Sterling Formations exposed near Homer, Kenai Peninsula, Alaska: U.S. Geological Survey Open-File Report 75-383, 239 p., 1 sheet.

Barnes, F.F., and Cobb, E.H., 1959, Geology and coal resources of the Homer District, Kenai coal field, Alaska: U.S. Geological Survey Bulletin 1058-F, p. 217-260, 12 plates.

Boss, R.F., Lennon, R.B., and Wilson, R.W., 1976, Middle Ground Shoal oil field, Alaska, *in* Braunstein, J., ed., North American Oil and Gas Fields: American Association of Petroleum Geologists Memoir 24, p. 1-22.

Bradley, D.C., Parrish, R., Clendenen, W., Lux, D., Layer, P.W., Heizler, M., and Donley, D.T., 2000, New geochronological evidence for the timing of Early Tertiary ridge subduction in southern Alaska: U.S. Geological Survey Professional Paper 1615, p. 5–21.

Calderwood, K.W., and Fackler, W.C., 1972, Proposed stratigraphic nomenclature for Kenai Group, Cook Inlet basin, Alaska: American Association of Petroleum Geologists Bulletin, v. 56, p. 739–754.

Claypool, G.E., Threlkeld, C.N., and Magoon, L.B., 1980, Biogenic and thermogenic origins of natural gas in Cook Inlet basin, Alaska: American Association of Petroleum Geologists Bulletin, v. 64, p. 1,131–1,139.

Dallegge, T.A., and Layer, P.W., 2004, Revised chronostratigraphy of the Kenai Group from $^{40}Ar/^{39}Ar$ dating of low-potassium bearing minerals, Cook Inlet basin, Alaska: Canadian Journal of Earth Science, v. 41, p. 1,159–1,179.

Detterman, R.L., and Hartsock, J.K, 1966, Geology of the Iniskin–Tuxedni Region, Alaska: U.S. Geological Survey Professional Paper 512, 78 p., 6 plates.

Dickinson, W.R., 1995, Forearc basins, *in* Busby, C.J., and Ingersoll, R.J., eds., Tectonics of Sedimentary Basins: Blackwell Science, p. 221–261.

Fisher, M.A., and Magoon, L.B., 1978, Geologic framework of lower Cook Inlet, Alaska: American Association of Petroleum Geologists Bulletin, v. 62, p. 373–402.

Flores, R.M., and Stricker, G.D., 1992, Some facies aspects of the upper part of the Kenai Group, southern Kenai Peninsula, Alaska, *in* Bradley, D.C., and Dusel-Bacon, C., eds., Geologic Studies in Alaska by the U.S. Geological Survey, 1991: U.S. Geological Survey Bulletin 2041, p. 160–170.

Flores, R.M., and Stricker, G.D., 1993, Reservoir framework architecture in the Clamgulchian type section (Pliocene) of the Sterling Formation, Kenai Peninsula, Alaska, *in* Dusel-Bacon, C., and Till, A.B., eds., Geologic Studies in Alaska by the U.S. Geological Survey, 1992: U.S. Geological Survey Bulletin 2068, p. 118–129.

Flores, R.M., Stricker, G.D., and Roberts, S.B., 1994, Miocene coal-bearing strata of the Tyonek Formation—Braided stream deposits in the Chuit Creek–Chuitna River drainage basin, southern Alaska, *in* Till, A.B., and Moore, T.E., eds., Geologic Studies in Alaska by the U.S. Geological Survey, 1993: U.S. Geological Survey Bulletin 2107, p. 95–114.

Flores, R.M., Stricker, G.D., and Stiles, R.B., , 1997, Tidal influence on deposition and quality of coals in the Miocene Tyonek Formation, Beluga coal field, upper Cook Inlet, Alaska, *in* Dumoulin, J.A., and Gray, J.E., eds., Geologic Studies in Alaska by the U.S. Geological Survey, 1995: U.S. Geological Survey Professional Paper 1574, p. 137–156.

Flores, R.M., Stricker, G.D., and Kinney, S.A., 2004, Alaska coal geology, resources, and coalbed methane potential: U.S. Geological Survey Digital Data Series 77, 125 p.

Gillis, R.J., Herriott, T.M., Shellenbaum, D.P., Mauel, D.J., Wartes, M.A., Decker, P.L., Freeman, L.K., LePain, D.L., Gregerson, L.S., and Elliott, B.A., *in preparation*, Interpretive bedrock geologic map of the south-central Tyonek Quadrangle, Alaska, 1:63,360-scale: Alaska Division of Geological & Geophysical Surveys Report of Investigation.

Hayes, J.B., Harms, J.C., and Wilson, T.W, 1976, Contrasts between braided and meandering stream deposits, Beluga and Sterling Formations (Tertiary), Cook Inlet, Alaska, *in* Miller, T.P., ed., Recent and Ancient Sedimentary Environments in Alaska: Alaska Geological Society Symposium Proceedings, Anchorage, Alaska, 27 p.

Haeussler, P.J., Bruhn, R.L., and Pratt, T.L., 2000, Potential seismic hazards and tectonics of the upper Cook Inlet basin, Alaska, based on analysis of Pliocene and younger deformation: Geological Society of America Bulletin, v. 112, p. 1,414–1,429.

Helmold, K.P., LePain, D.L., Wilson, M.D., and Peterson, C.S., 2013, Petrology and reservoir potential of Tertiary and Mesozoic sandstones, Cook Inlet, Alaska—A preliminary analysis of outcrop samples collected during 2007–2010 field seasons: Alaska Division of Geological & Geophysical Surveys Preliminary Interpretive Report 2013-5, 34 p.

Hite, D.M., and Stone, D.M., 2013, A history of oil and gas exploration, discovery and future potential—Cook Inlet basin, south-central Alaska, *in* Stone, D.M., and Hite, D.M., eds., Oil and Gas Fields of the Cook Inlet Basin, Alaska: Association of American Petroleum Geologists Memoir 104, p. 1–35.

Kirschner, C.E., and Lyon, C.A., 1973, Stratigraphic and tectonic development of Cook Inlet petroleum province, in Pitcher, M.G., ed., Arctic Geology: American Association of Petroleum Geologists Memoir 19, p. 396–407.

LePain, D.L., Wartes, M.A., McCarthy, P.J., Stanley, R.G., Silliphant, L.J., Helmold, K.P., Shellenbaum, D.P., Gillis, R.J., Peterson, S., Mongrain, Jacob, and Decker, Paul, 2008, Tertiary depositional systems in upper Cook Inlet, Alaska—Influence of fluvial style on reservoir geometries and stratigraphic trap potential [abs.]: American Association of Petroleum Geologists 2008 Annual Convention and Exhibition, abstracts volume, p. 119.

LePain, D.L., Wartes, M.A., McCarthy, P.J., Stanley, R.G., Silliphant, L.J., Peterson, Shaun, Shellenbaum, D.P., Helmold, K.P., Decker, P.L., Mongrain, Jacob, and Gillis, R.J., 2009, Facies associations, sand body geometry, and depositional systems in Late Oligocene–Pliocene strata, southern Kenai Peninsula, Cook Inlet, Alaska—Report on progress during the 2006–07 field season, *in* LePain, D.L., ed., Preliminary results of recent geologic investigations in the Homer–Kachemak Bay area, Cook Inlet Basin—Progress during the 2006–2007 field season: Alaska Division of Geological & Geophysical Surveys Preliminary Interpretive Report 2009-8A, p. 1–97.

LePain, D.L., Stanley, R.G., Helmold, K.P., and Shellenbaum, D.P., 2013, Geologic framework and petroleum systems of Cook Inlet basin, south-central Alaska, *in* Stone, D.M., and Hite, D.M., eds., Oil and Gas Fields of the Cook Inlet Basin, Alaska: American Association of Petroleum Geologists Memoir 104, p. 37–116.

Lillis, P.G., and Stanley, R.G., 2011, Petroleum generation modeling for Cook Inlet basin, Alaska [abs.]: American Association of Petroleum Geologists, Pacific Section Annual Meeting, p. 72.

Magoon, L.B., 1994, Tuxedni–Hemlock(!) petroleum system in Cook Inlet, Alaska, U.S.A., *in* Magoon, L.B., and Dow, W.G., eds., The Petroleum System—From Source to Trap: American Association of Petroleum Geologists Memoir 60, p. 359–370.

Magoon, L.B., and Anders, D.E., 1992, Oil-to-source-rock correlation using carbon-isotopic data and biological marker compounds, Cook Inlet—Alaska Peninsula, Alaska, *in* Moldowan, J.M., Albrecht, Pierre, and Philp, R.P., eds., Biological markers in sediments and petroleum: Englewood Cliffs, N.J., Prentice-Hall, p. 241–274.

Magoon, L.B., and Kirschner, C.E., 1990, Alaska onshore national assessment program—Geology and petroleum resource potential of six onshore Alaska provinces: U.S. Geological Survey Open-File Report 88-450T, 47 p.

Magoon, L.B., Adkison, W.L., and Egbert, R.M., 1976, Map showing geology, wildcat wells, Tertiary plant fossil localities, K-Ar age dates, and petroleum operations, Cook Inlet area, Alaska: Miscellaneous Investigations Series Map I-1019, 2 sheets, 1:250,000 scale.

Mongrain, Jacob, 2012, Depositional systems, paleoclimate, and provenance of the Late Miocene to Pliocene Beluga and Sterling Formations, Cook Inlet forearc basin: Fairbanks, University of Alaska Fairbanks, unpublished Ph.D. thesis.

Nokleberg, W.J., Parfenov, L.M., Monger, J.W.H., Norton, I.O., Khanchuk, A.L., Stone, D.B., Scholl, D.W., and Fujita, K., 1998, Phanerozoic tectonic evolution of the circum-Pacific: U.S. Geological Survey Open-file Report 98-754, 125 p.

Pettijohn, F.J., and Potter, P.E., 1964, Atlas and Glossary of Primary Sedimentary Structures: Springer-Verlag, New York, 370 p.

Plafker, George, Moore, J.C., and Winkler, G.R., 1994, Geology of the southern Alaska margin, *in* Plafker, George, and Berg, H.G., eds., The Geology of Alaska: Geological Society of America, Geology of North America, v. G-1, p. 389–450.

Rawlinson, S.E., 1984, Environments of deposition, paleocurrents, and provenance of Tertiary deposits along Kachemak Bay, Kenai Peninsula, Alaska: Sedimentary Geology, v. 38, p. 421–442.

Reger, R.D., 1979, Bluff Point landslide, a massive ancient rock failure near Homer, Alaska, *in* Alaska Division of Geological & Geophysical Surveys, Short Notes on Alaskan Geology, 1978: Alaska Division of Geological & Geophysical Surveys Geologic Report 61B, p. 5–9. doi:10.14509/409

Reinink-Smith, L.M., 1995, Tephra layers as correlation tools of Neogene coal-bearing strata from the Kenai Lowland, Alaska: Geological Society of America Bulletin, v. 107, p. 340–353.

Rioux, Matthew, Mattinson, James, Hacker, Bradley, Kelemen, Peter, Blusztajn, Jurek, Hanghøj, Karen, and Gehrels, George, 2010, Intermediate to felsic middle crust in the accreted Talkeetna arc, the Alaska Peninsula and Kodiak Island, Alaska: An analogue for low-velocity middle crust in modern arcs: Tectonics, v. 29, no. 3, 17 p. doi:10.1029/2009TC002541

Shellenbaum, D.P., Gregersen, L.S., and Delaney, P.R., 2010, Top Mesozoic unconformity depth map of the Cook Inlet Basin, Alaska: Alaska Division of Geological & Geophysical Surveys Report of Investigation 2010-2, 1 sheet, scale 1:500,000. doi:10.14509/21961

Smith, G.A., and Lowe, D.R., 1991, Lahars—Volcano–hydrologic events and deposition in the debris flow–hyperconcentrated flow continuum, in Fisher, R.V., and Smith, G.A., eds., Sedimentation in Volcanic Settings: SEPM Special Publication 45, p. 59-70.

Swenson, R.F., 2003, Introduction to Tertiary tectonics and sedimentation in the Cook Inlet basin, *in* Dallegge, T.A., compiler, 2001 guide to the petroleum geology and shallow gas potential of the Kenai Peninsula, Alaska: Alaska Division of Geological & Geophysical Surveys Miscellaneous Publication 128, p. 10–19.

Thomas, C.P., Doughty, T.C., Faulder, D.D., and Hite, D.M., 2004, South-central Alaska natural gas study final report: U.S. Department of Energy, National Energy Technology Laboratory, Arctic Energy Office Contract DE-AM26-99FT40575, 207 p., available at http://fossil.energy.gov/programs/oilgas/publications/

Todd, E., Jones, J.V., Karl, S., Ayuso, R.A., Bradley, D.C., Box, S.E., and Haeussler, P.J., 2014, Magmatic responses to Late Cretaceous through Oligocene tectonic evolution of the western Alaska Range: EOS Transactions, American Geophysical Union, Fall Meeting, v. 32, p. B-06.

Triplehorn, D.M., Turner, D.L., and Naeser, C.W., 1977, K-Ar and fission-track dating of ash partings in coal beds from the Kenai Peninsula, Alaska—A revised age for the Homerian Stage–Clamgulchian Stage boundary: Geological Society of America Bulletin, v. 88, p. 1,156–1,160.

Trop, J.M., and Ridgway, K.D., 2007, Mesozoic and Cenozoic tectonic growth of southern Alaska—A sedimentary basin perspective, in Ridgway, K.D., Trop, J.M., Glen, J.M.G., and O'Neill, J.M., eds., Tectonic Growth of a Collisional Continental Margin—Crustal Evolution of Southern Alaska: Geological Society of America Special Paper 431, p. 55–94.

Trop, J.M., Szuch, D.A., Rioux, Matthew, and Blodgett, R.B., 2005, Sedimentology and provenance of the Upper Jurassic Naknek Formation, Talkeetna Mountains, Alaska—Bearings on the accretionary tectonic history of the Wrangellia composite terrane: Geological Society of America Bulletin, v. 117, p. 570–588.

Turner, D.L, Triplehorn, D.M., Naeser, C.W., and Wolfe, J.A., 1980, Radiometric dating of ash partings in Alaskan coal beds and upper Tertiary paleobotanical stages: Geology, v. 8, p. 92–96.

U.S. Geological Survey, 2011, Assessment of undiscovered oil and gas resources of the Cook Inlet region, south-central Alaska: USGS Fact Sheet 2011-3068.

Wang, J., Newton, C.R., and Dunne, L., 1988, Late Triassic transition from biogenic to arc sedimentation on the Peninsular terrane—Puale Bay, Alaska Peninsula: Geological Society of America Bulletin, v. 100, p. 1,466–1,478.

Wilson, F.H., Hults, C.P., Schmoll, H.R., Haeussler, P.J., Schmidt, J.M., Yehle, L.A., and Labay, K.A., 2012, Geologic map of the Cook Inlet region, Alaska: U.S. Geological Survey Scientific Investigations Map 3153, 75 p., 2 map sheets, scale 1:250,000.

Wolfe, J.A., Hopkins, D.M., and Leopold, E.B., 1966, Tertiary stratigraphy and paleobotany of the Cook Inlet region, Alaska: U.S. Geological Survey Professional Paper 398-A, 29 p., 2 plates.